

TECHNICAL NOTE

Aqueduct 4.0: Updated decision-relevant global water risk indicators

Samantha Kuzma, Marc F.P. Bierkens, Shivani Lakshman, Tianyi Luo, Liz Saccoccia, Edwin H. Sutanudjaja, and Rens Van Beek

CONTENTS

Introduction.....	2
Water risk framework	2
Hydrological model	4
Future projections.....	9
Indicators	10
Country and state aggregation.....	33
Grouped and overall water risk.....	35
Limitations.....	36
Appendix A.....	39
Appendix B.....	40
Appendix C	41
Appendix D	44
Endnotes.....	45
References.....	46
Acknowledgements.....	51
About the authors.....	51

Technical notes document the research or analytical methodology underpinning a publication, interactive application, or tool.

Suggested Citation: Kuzma, S., M.F.P. Bierkens, S. Lakshman, T. Luo, L. Saccoccia, E. H. Sutanudjaja, and R. Van Beek. 2023. "Aqueduct 4.0: Updated decision-relevant global water risk indicators." Technical Note. Washington, DC: World Resources Institute. Available online at: doi.org/10.46830/wrtn.23.00061.

ABSTRACT

Water is essential to the progress of human societies. Food production, electricity generation, and manufacturing, among other things, all depend on it. However, many decision-makers lack the technical expertise to fully understand hydrological information.

We present Aqueduct 4.0, the latest iteration of WRI's water risk framework designed to translate complex hydrological data into intuitive indicators of water-related risk. We curated 13 water risk indicators—spanning quantity, quality, and reputational concerns—into a comprehensive framework. Each indicator is sourced from an open-source, peer-reviewed data provider and then transformed to normalized risk score based on the severity of the water challenge. For 5 of the 13 indicators, we used a global hydrological model called PCR-GLOBWB 2 to generate novel datasets on sub-basin water supply and use.

We also used the PCR-GLOBWB 2 model to project future sub-basin water supply, demand, stress, depletion, and variability using CMIP6 climate forcings. The projections centered around three periods (2030, 2050, and 2080) under three future scenarios (business-as-usual SSP 3 RCP 7.0, optimistic SSP 1 RCP 2.6, and pessimistic SSP 5 RCP 8.5).

The normalized indicator scores have been aggregated by category (quantity, quality, reputational, and overall) into composite risk scores using sector-specific weighting schemes. In addition, select sub-basin scores have been aggregated into country and provincial administrative boundaries using a weighted average approach, where sub-basins with more demand have a higher influence over the final administrative score.

The main audience for this technical note includes users of the Aqueduct tool, for whom the short descriptions on the tool and in the metadata document are insufficient. Key elements of Aqueduct, such as overall water risk, cannot be directly measured and therefore are not validated. Aqueduct remains primarily a prioritization tool and should be augmented by local and regional deep dives.

INTRODUCTION

Background

WRI's Aqueduct™ information platform compiles advances in hydrological modeling, remotely sensed data, and published data sets into a freely accessible online platform.

Since its inception in 2011, the Aqueduct information platform has informed companies, governments, and nongovernmental organizations (NGOs) about water-related risks. Since then, the data have been updated regularly, making them comparable on a global scale and accessible to decision-makers worldwide. The Aqueduct information platform contains the following online tools:

- Aqueduct Water Risk Atlas
- Aqueduct Food
- Aqueduct Floods
- Aqueduct Country Rankings

This technical note covers the development of the Aqueduct 4.0 framework and serves as the basis of the updated Aqueduct Water Risk Atlas and Country Rankings online tools.

The updated framework, database, and associated tools improve one of the most widely used and respected water risk frameworks. We continue to build on years of experience applying and standardizing these concepts within the water community, while presenting the latest advancements in hydrological data and climate science.

Structure and scope of this technical note

This technical note will first introduce the updated water risk framework ("Water risk framework"). Many indicators in the framework are based on updated inputs to a global hydrological model, which is covered in "Hydrological model" and "Future projections" (baseline and future, respectively). In "Indicators" we discuss how the hydrological data is transformed into Aqueduct water risk indicators. "Country and state aggregation" and "Grouped and overall water risk" cover how the individual indicators are aggregated into administrative-level scores and grouped (categorical risk) scores. "Limitations" lists key limitations.

WATER RISK FRAMEWORK

Overview

The water risk framework follows a composite index approach and allows multiple water-related risks to be combined.

There are three hierarchical levels, as can be seen in Figure 1. We start with 13 indicators covering various types of water risk. We then group the indicators and calculate the grouped water risk scores (composite score) using default, industry-defined, or user-defined weighting schemes. Finally, the three groups are combined into a single overall water risk score.

The rationale for creating a water risk framework is described in WRI's earlier publication: "Aqueduct Water Risk Atlas" (Reig et al. 2013):

This [water risk] framework organizes indicators into categories of risk that allow the creation of a composite index that brings together multiple dimensions of water-related risk into comprehensive aggregated scores. By providing consistent scores across the globe, the Aqueduct Water Risk Atlas enables rapid comparison across diverse aspects of water risk. . . .

The Aqueduct Water Risk Framework enables users to study indicators individually or collectively, as well as to quantify and compare a variety of multidimensional water-related measures.

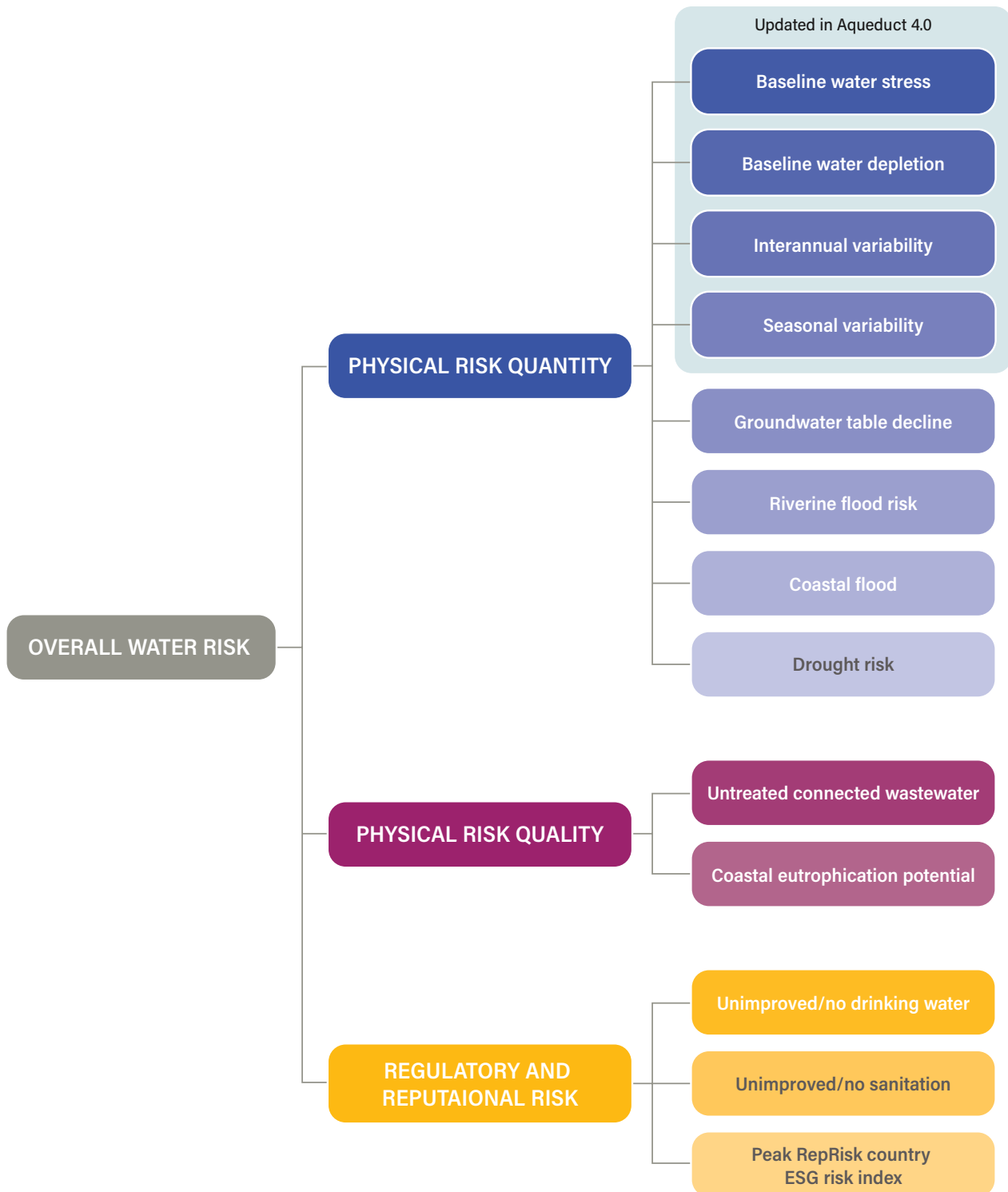
We selected the 13 indicators in Aqueduct 4.0 in three steps:

- We reviewed literature on relevant water issues, existing water indicators, and data sources.
- We evaluated potential data sources through a comparative analysis of their spatial and temporal coverage, granularity, relevance to water users, consistency, and credibility of sources.
- We consulted with industry, public sector, and academic water experts.

We applied the following three principal criteria in selecting indicators:

- They should cover the full breadth of water-related risks, while minimizing overlap and potential confusion resulting from an overabundance of indicators.
- They should be actionable in the context of private and public sector decision-making.

Figure 1 | Overview of Aqueduct framework



Note: Baseline water stress, baseline water depletion, interannual variability, and seasonal variability use the new PCR-GLOWB2 data, described in "Hydrological model" and Appendix C.
 Source: WRI.

- They should comply with WRI's commitment to open data and transparency—allowing input data, code, and results to be publicly available ("WRI's Open Data Commitment" n.d.).

HYDROLOGICAL MODEL

Five of the 13 indicators in our framework are based on the data from a global hydrological model called PCR-GLOBWB 2. Readers interested only in the indicator definitions can proceed directly to "Indicators." In the present section, we describe how we have selected the hydrological model and processed its data for the baseline indicators of Aqueduct. For data sources used in Aqueduct's future projections, please refer to "Future projections."

From the model, we make use of water use, water supply, and groundwater data¹ to calculate water stress, water depletion, seasonal variability, interannual variability, and groundwater table decline (see Table 1).

Model selection

We considered several global hydrological models and selected the PCRaster Global Water Balance (PCR-GLOBWB 2) model (Wada et al. 2014; Sutanudjaja et al. 2018) over others, most notably Water Global Assessment and Prognosis (WaterGAP) (Müller Schmied et al. 2014; Eisner 2016) and Global Land Data Assimilation System (GLDAS) Phase 2 (Rodell et al. 2004). While these three are not the only global hydrological models available (Paul et al. 2021; Wang et al. 2021), they were short-listed because of their dynamic human-freshwater system modeling and their potential to be used for water target setting.

At the time the indicators were developed for Aqueduct 3.0 (2016–2019), GLDAS provided information until the year 2012, making it less relevant than PCR-GLOBWB 2 and WaterGAP, both of which could be run for more recent years. There are many similarities between PCR-GLOBWB 2 and WaterGAP. For example, both models run global hydrology and water resources on a global scale at a daily time step; integrate demand, withdrawal, and return flows² per time step; include reservoirs; and use kinematic wave routing of river water. However, PCR-GLOBWB 2 can couple to a global two-layer groundwater model (based on MODFLOW) to better represent groundwater flow (de Graaf et al. 2017). The code for PCR-GLOBWB 2 is open source and therefore aligned with WRI's Open Data Commitment ("WRI's Open Data Commitment" n.d.). For these reasons, WRI chose to continue to work with PCR-GLOBWB 2 and use it as the updated global hydrological model underpinning Aqueduct.

A description of the model itself and the settings used for Aqueduct 4.0 can be found in Appendix C. This includes references to the new input datasets used to run PCR-GLOBWB 2 for Aqueduct 4.0 compared to the run in 2019 for Aqueduct 3.0.

Model data used by Aqueduct

PCR-GLOBWB 2 is a global, gridded hydrological model. Each grid cell has a size of 5×5 arc minutes. This equates roughly to 10 kilometer (km) \times 10 km pixels, with any variation depending on the latitude. Aqueduct indicators are calculated using three PCR-GLOBWB 2 datasets: water use, water supply, and groundwater data (see Table 1).

Table 1 | Aqueduct indicators based on hydrological model output

AQUEDUCT INDICATOR	MODEL DATA USED		
	Water Use	Water Supply	Groundwater Heads
Water stress	✓	✓	
Water depletion	✓	✓	
Interannual variability		✓	
Seasonal variability		✓	
Groundwater table decline			✓

Note: Aqueduct indicators are calculated using the respective outputs of a hydrological model. For example, water depletion is calculated using water consumption and available blue water from the hydrological model.

Source: WRI.

WATER USE:

Aqueduct considers two metrics of water use: gross demand and net consumption. Gross demand³ is the maximum potential water required to meet sectoral demands, and net consumption is the portion of demand that is lost in use—evaporated or incorporated into a product—and not returned to the system (Gassert et al. 2014).

Gross demand and net consumption⁴ for four sectors: domestic, industrial, irrigation⁵, and livestock⁶. The (2 x 4=) 8 gridded data sets are available for each month between January 1960 and December 2019.

WATER SUPPLY:

Aqueduct defines supply as available blue water—the total amount of renewable freshwater available to a sub-basin with upstream consumption removed (Gassert et al. 2014). We compute available blue water as internal sub-basin runoff plus the accumulated water flowing into the sub-basin from upstream, where upstream consumption is already removed (i.e., discharge) (Gassert et al. 2014). This includes freshwater from the following sources: surface flow, interflow⁷, and groundwater recharge.

Internal runoff⁸ monthly at each grid cell between January 1960 and December 2019.

Discharge⁹ monthly at each grid cell between January 1960 and December 2019.

GROUNDWATER HEADS:

Groundwater heads for each month and each grid cell between January 1990 and December 2014. These have been obtained from the 5 arc minute two-layer global groundwater model of de Graaf et al (2017) coupled to PCR-GLOBWB 2. Note: this dataset has not been rerun since its original release in 2019.

Processing model data

To make the model data suitable for the Aqueduct indicator calculation, we further processed the data by spatial and temporal aggregation.

- Spatial aggregation. Water use and water supply are aggregated to hydrological sub-basins. Groundwater heads are aggregated to aquifers.
- Temporal aggregation. We apply statistical methods to the output time series to get a representative value for the recent situation, while correcting for annual anomalies.

Spatial aggregation

Grid cells are not an appropriate spatial unit to use as input for the Aqueduct indicators. For water stress, water depletion, seasonal variability, and interannual variability, the preferred spatial units are hydrological sub-basins (Gassert et al. 2014). For groundwater table decline, the preferred spatial units are aquifers.

HYDROLOGICAL SUB-BASINS:

A hydrological basin is an area that drains at a single point to an outlet such as a river, ocean or inland lake. Each basin can be divided into smaller sub-basins at the confluence of two streams (Lehner and Grill 2013). The assumption is that within each hydrological sub-basin, water resources are pooled. Water withdrawal is satisfied using the water resources available to the sub-basin.

Aqueduct 4.0 uses the HydroBASINS level 6 hydrological sub-basins for a few reasons, including the following:

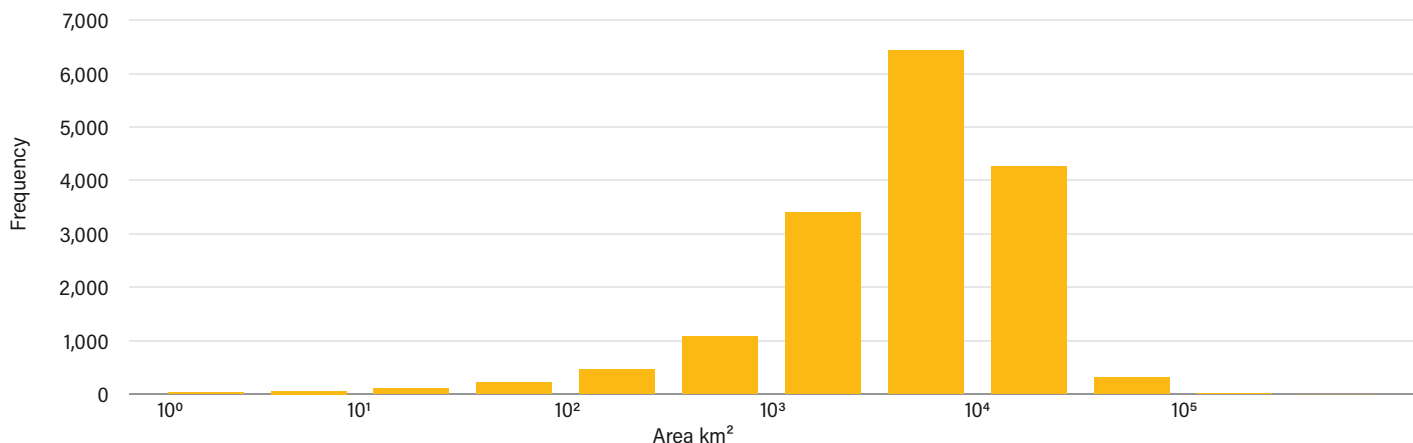
- HydroBASINS are used in other tools and databases, so comparing and collating data is easier.
- The HydroBASINS sub-basin data set contains 12 levels, ranging from large basins to small sub-basins. In the future, this hierarchical model will allow flexibility when combining additional data sets (Lehner and Grill 2013).

Of the 12 levels, we chose level 6 as the appropriate size of the sub-basins. Water demand is often satisfied with water from a nearby or slightly more distant source. The average distance from source to destination of water supply is the main selection criterion of the appropriate HydroBASINS level. The goal is to select a level large enough to minimize the nonnatural effect of transfers of water (“inter-basin transfer”)¹⁰ and small enough to capture meaningful local variations.

Based on limitations, primarily the lack of comprehensive local level inter-basin transfer data in PCR-GLOBWB 2, HydroBASINS level 6 is deemed the most appropriate sub-basin level for Aqueduct 4.0 analysis. For perspective, HydroBASINS level 6 has a median area per sub-basin¹¹ of 5,318 km² (roughly the size of the U.S. state of Delaware or twice the size of Luxembourg). The distribution of sub-basin areas is depicted in Figure 2.

PCR-GLOBWB 2 and HydroBASINS level 6 both assume a strictly convergent flow. This means that it cannot model bifurcations. This is an issue in delta regions, where rivers tend to split. To address this issue, we have identified delta sub-basins and merged them. The methodology is explained in Appendix D.

Figure 2 | Area distribution of HydroBASIN Level 6



Source: WRI.

AQUIFERS

Groundwater head data are aggregated to groundwater aquifers (BGR and UNESCO 2008). This data set of global aquifers is selected because it has global coverage and is used in the previous versions of Aqueduct.

STEP 1: SPATIAL AGGREGATION OF WATER USE

Sectoral gross demand and net consumption are aggregated to HydroBASINS level 6. First, the data are resampled from 5×5 arc minute to 1×1 arc minute¹². Then, the data, which are in flux (m/month), are converted to volume (million m^3/month) by multiplying each grid by its cell area (m^2) and dividing by a million. Finally, we sum the gridded volume per sub-basin.

STEP 2: SPATIAL AGGREGATION OF WATER SUPPLY

Supply—also known as available blue water—is also aggregated to HydroBASIN level 6. Available blue water equals the internal sub-basin runoff plus the accumulated water flowing into the sub-basin from upstream, where upstream consumption is already removed (i.e., discharge) (Gassert et al. 2014).

First, we use the internal runoff to find the renewable water supply within each sub-basin—that is, internal catchment supply *before* consumption is removed. Like the demand data, runoff is available as a flux, and so we follow the same spatial aggregation process as demand.

Next, we use discharge to account for the accumulated water flowing into each sub-basin, with upstream consumption already removed. Discharge is the rate (m^3/sec) of water flow-

ing through a river channel, not a flux, and therefore requires a different spatial aggregation technique.

To turn discharge into inflow, we first must identify inflow and outflow points¹³ for each sub-basin using the PCR-GLOBWB 2 local drainage direction (LDD¹⁴) network (see Appendix C). Normally, a hydrologically sound sub-basin would have just one inflow and one outflow point; however, due to the rasterization¹⁵ of the sub-basins and the mismatched resolutions between PCR-GLOBWB 2's digital elevation model and the HydroBASIN sub-basins¹⁶, we have numerous inflow and outflow points per sub-basin (see Figure 3). Some of these discharge flow points are considered “false”¹⁷, meaning the stream temporarily leaves or enters the sub-basin. In each sub-basin, all flow points satisfy this condition:

$$\text{true outflow} = \text{all discharge inflow} - \text{false discharge outflow} + \text{internal runoff} - \text{internal consumption}$$

This translates to the definition of available blue water by removing the internal consumption term:

$$\text{available blue water} = \text{all discharge inflow} - \text{false discharge outflow} + \text{internal runoff}$$

We sum the discharge values at all (true and false) inflow points and subtract the discharge values from the false outflow points (white and purple arrows in Figure 3, respectively) to calculate the accumulated water flowing into the sub-basin. We then add internal runoff to estimate available blue water.

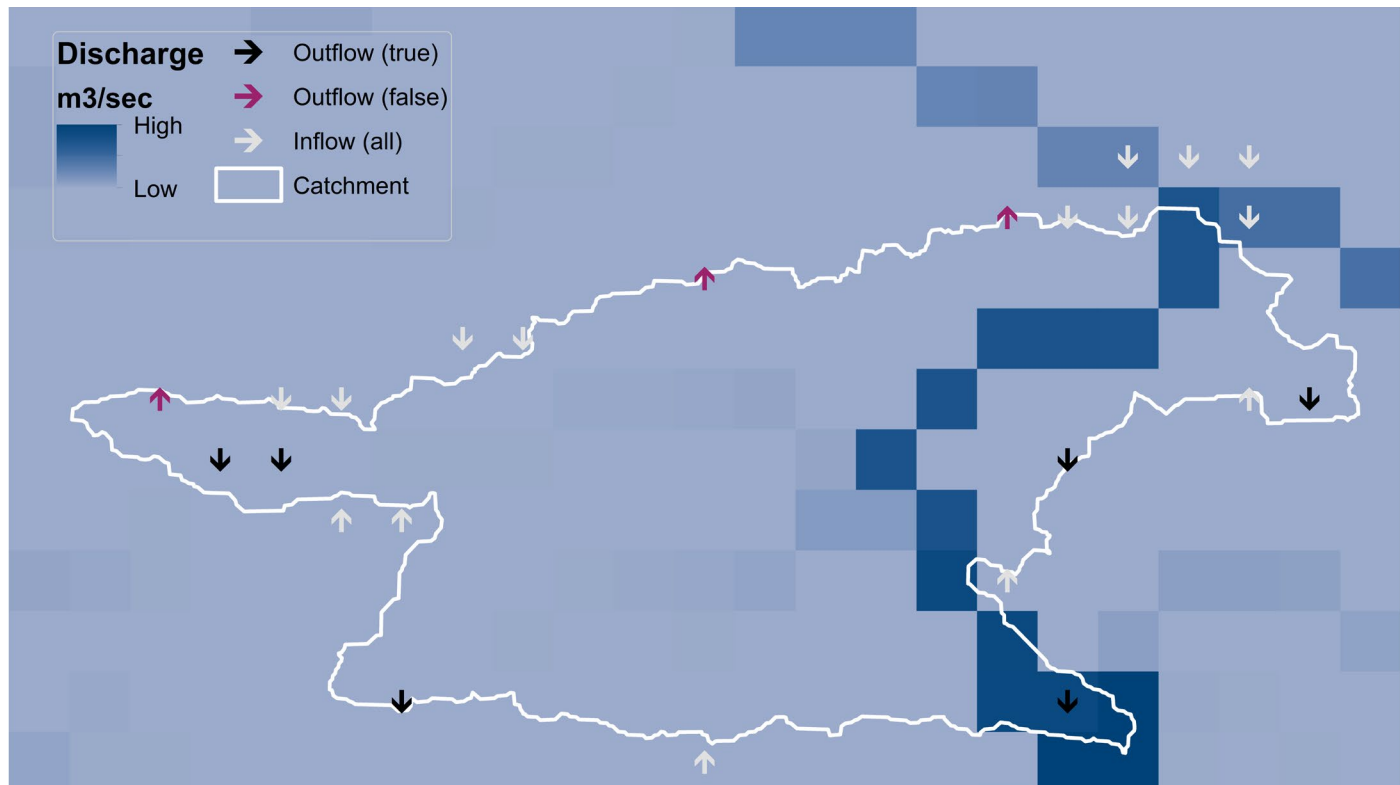
Temporal aggregation

One of the advantages of the Aqueduct framework is its ease of use. Although time series provide detailed insights, for a prioritization method and combined framework, summary indicators are preferred. Aqueduct provides **chronic** water risk information. This is very different from near-real-time water risk information or a historical assessment. Ideally, each indicator is representative of the relative time period—be that baseline or future—with anomalies (the exception being the variability indicators, in which anomalies are intentionally captured).

We apply temporal aggregation steps to convert historical time series into useful input for the baseline indicator calculations. Aqueduct 4.0's baseline represents a 40-year period (1979–2019)¹⁸. For water stress and depletion, the long-term trends are extracted from the noise using the methodology below. For seasonal and interannual variability, the raw time series are used.

Temporal aggregation for future projections can be found “Processing model data” in the next section. Groundwater head data are processed separately; see “Groundwater table decline” in the “Indicators” section for more information.

Figure 3 | Example of discharge inflow and outflow points



Source: Authors.

STEP 1: TOTAL WATER USE

We calculate the total gross demand and total net consumption by summing up the four sectors (domestic, industrial, irrigation, and livestock) for each sub-basin and month (January 1979–December 2019). The results are two time series: Gross total demand and net total consumption for January 1979–December 2019 for each sub-basin.

STEP 2: SPLIT MONTHS

We then break up the time series into one series for each month. This yields time series of all Januaries between 1979 and 2019, all Februaries between 1979 and 2019, and so on to all Decembers between 1979 and 2019. We do this for total gross demand, total net consumption, and available blue water.

STEP 3: REGRESSION

In most sub-basins, the water use data follow a clearly increasing trend. This is caused by increases in underlying drivers such as growth in population and gross domestic product (GDP). In

addition, both the demand data¹⁹ and supply data can be erratic. We try to reduce noise while keeping an accurate representation of the present value based on the long-term trend. We first smooth the data by applying a trailing moving average with a window size of 10 years. We then run a Theil-Sen regression²⁰ on the moving average to capture the trend. We select the point intersecting with our target year—2019—to represent the baseline. The independent variable is time (year), and the dependent variable is either gross total withdrawal, net total withdrawal, or available blue water.

Additionally, we restrict the predicted value to the minimum and maximum range of the 10-year moving average window values. The predicted value can never exceed the maximum of the 10-year window values or be lower than the minimum of the 10-year window functions.

We opted for a window size of 10 years to capture longer climatic and socioeconomic trends while filtering annual anomalies. The temporal aggregation steps 1 through 3 for an example sub-basin are shown in Figure 4.

STEP 4: MASK ARID AND LOW WATER USE SUB-BASINS

Aqueduct indicators require robust data as inputs.²¹ Sub-basins where data are sparse or very close to zero should

therefore be handled separately. We identified those sub-basins using two criteria with thresholds taken from Aqueduct 2.1 (Gassert et al. 2014):

A sub-basin is “arid” if annual baseline available water < 0.03 meters per year (m/yr)

A sub-basin is “low water use” if annual baseline gross total withdrawal < 0.012 m/yr

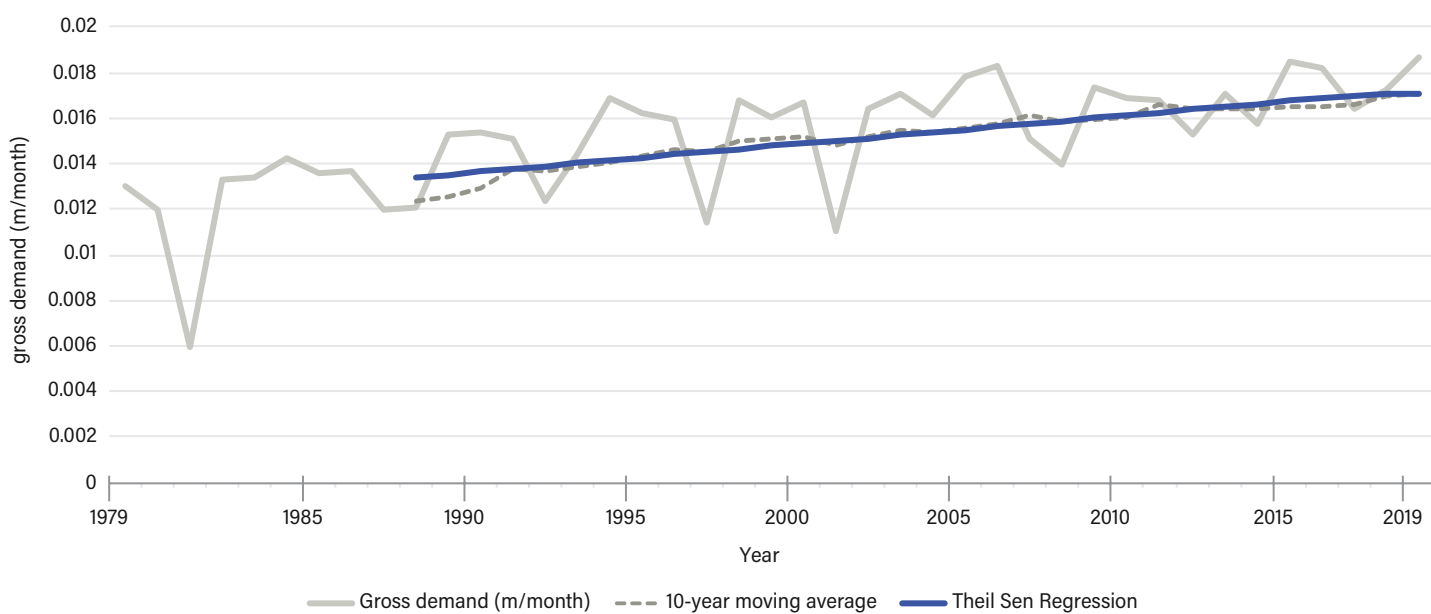
Data must be below both the arid and low water use thresholds to be masked. Monthly data is masked using the annual arid and low water use categories.

Processed water use and water supply

After applying the spatial and temporal aggregation steps, we have estimates of gross demand (ww), net consumption (wn), and available blue water (ba) for each sub-basin.

Delta regions and arid and low water use sub-basins will be treated accordingly in the indicator calculation. We use the aggregated time series of gross total withdrawal, net total withdrawal, and available water to calculate water stress, water depletion, seasonal variability, and interannual variability.

Figure 4 | Theil-Sen regression for gross demand on a 10-year moving average window for July in an example basin (Erbo Sub-basin [216041])



Source: Authors.

FUTURE PROJECTIONS

The availability of and competition for water resources around the world will be affected by climate change, population growth, and economic development. This analysis complements our baseline water risk data by providing information on future water availability that is relevant for long-term planning, adaptation, and investment by both the private and public sectors.

This section details the methodology used to develop global estimates of water supply (available blue water), water use (gross demand and net consumption), water stress (the ratio of demand to supply), water depletion (the ratio of consumption to supply), interannual variability, and seasonal (intra-annual) variability for three 30-year periods centered on milestone years 2030, 2050, and 2080. Projections of climate variables are driven primarily by general circulation models from the Coupled Model Intercomparison Project phase 6 (CMIP6) project, and socioeconomic variables are based on the Shared Socioeconomic Pathways database from the International Institute for Applied Systems Analysis.

Model data used by Aqueduct

The Aqueduct Future Projections are based on a new dataset called PCR-GLOWB-based hydrological projection of future global water states with CMIP 6 (HYPFLOWSCI6) (Sutanudjaja et al. 2023). They use the same model structure and classes of data to define water use and supply as the baseline, except they are created using different climate forcing data and cover greater time periods. HYPFLOWSCI6 uses climate forcing data from multiple future scenarios of socioeconomic and climate conditions, which are each run through five separate climate models.

SOCIOECONOMIC AND CLIMATE SCENARIOS:

Estimates of each indicator are developed for three socio-economic and climate scenarios used in CMIP6 (SSP1–2.6, SSP3–7.0, and SSP5–8.5). Shared socioeconomic pathways (SSPs), indicated by the first number in each scenario (1, 3, and 5), describe alternative futures of societal development and water use. The second number in each scenario (2.6, 7.0, and 8.5) indicates the level of radiative forcing (W m^{-2}) through 2100. These drive the climate factors in general circulation models (GCMs). The SSP pathways were used to project future water use, while the SSP/RCP combined pathways were used to project future water supply.

SSP1–2.6 represents an “optimistic” scenario limiting the rise in average global surface temperatures by 2100 to 1.3°C to 2.4°C

compared to preindustrial levels (1850–1900) (Arias et al. 2021). SSP1 is characterized by sustainable socioeconomic growth: stringent environmental regulations and effective institutions, rapid technological change and improved resource efficiency, and low population growth (Wada et al. 2016). SSP3–7.0 represents a “business as usual” scenario with temperatures increasing by 2.8°C to 4.6°C by 2100. SSP3 is a socioeconomic scenario characterized by regional competition and inequality, including slow economic growth, weak governance and institutions, low investment in the environment and technology, and high population growth, especially in developing countries. SSP5–8.5 represents a “pessimistic” scenario with temperature increases up to 3.3°C to 5.7°C . SSP5 describes fossil-fueled development: rapid economic growth and globalization powered by carbon-intensive energy, strong institutions with high investment in education and technology but a lack of global environmental concern, and the population peaking and declining in the 21st century. Each scenario has varying effects on water availability in different parts of the world.

GENERAL CIRCULATION MODELS (GCMS):

For each scenario, we ran five GCMs to account for the uncertainty in climate models: GFDL-ESM4, IPSL-CM6A-LR, MPI-ESM1–2-HR, MRI-ESM2-0, and UKESM1-0-LL. The five GCMs were bias-corrected²² toward the observed climate forcing data used for the baseline (Lange 2021, Hempel et al. 2013). They were chosen because they represent a span of temperature–precipitation variations (e.g., cold-wet). These five variations provided a good sample size for model uncertainty given our computational limitations²³. GCM data are converted into PCR-GLOWB inputs using the methodology described in Sutanudjaja et al. (2023). GCM data are prepared for both the historic time period (1960–2014) and the three future scenarios (2015–2100, each). In all, there are 5 historical runs and (5 x 3=) 15 future runs.

Processing model data

To make the model data suitable as input for the Aqueduct indicator calculation for future projections, we again process the data by spatial and temporal aggregations.

Spatial aggregation

For each future indicator, we aggregate water use and water supply to HydroBASINS level 6 hydrological sub-basins using the same methodology applied to the baseline (see under “Hydrological model”).

Temporal aggregation

We also follow the baseline methodology (see under “Hydrological model”) to temporally aggregate the future projections time series of water supply, demand, and consumption to our milestone years: we smooth the data using a 10-year trailing moving average and isolate the trend using a Theil-Sen regression. The only difference is the time periods used:

- 2014: 1960–2014 (historic GCM data)
- 2030: 2015–2045 (future GCM data)
- 2050: 2035–2065 (future GCM data)
- 2080: 2065–2095 (future GCM data)

We select the regressed value for each milestone year. We perform this step for each month in order to generate our annual results.

BIAS CORRECTION:

Each GCM uses unique estimates of climate under a given scenario spanning from the pre-industrial age to the year 2100, meaning that historical GCM climate forcing data may deviate from what actually happened. To correct this, we must adjust the future monthly GCM data to our monthly baseline data—specifically, total gross demand, total net consumption, and available blue water. We perform this bias correction in two steps. First, we calculate the change between the future GCM output and the historical GCM output:

$$\text{Adjusted Future Data} = \text{Baseline} + (\text{Future GCM} - \text{Historic GCM})$$

Processed water use and water supply

After applying the spatial and temporal aggregation steps and the bias correction, we have 2030, 2050, and 2080 estimates of total gross demand, total net consumption, and available blue water for each GCM for each scenario. We use these data to calculate future water stress, water depletion, seasonal variability, and interannual variability using the indicator methodology outlined in “Indicators.” Then, we find the median, minimum, maximum, and standard deviation across the GCMs per scenario for each indicator. The median is used as the default representation for each scenario. We estimate the uncertainty of the GCM data by calculating the coefficient of variation of the five GCMs scores per indicator within each catchment (Luck et al. 2015).

Future projections limitations

Irrigation data projects crop extents using the IMAGE dataset, which ends in 2050 (Doelman et al. 2018). Therefore, crop extents beyond 2050 are assumed to remain static to the 2050 extent (though total irrigation demand may still fluctuate beyond 2050 due to varying climatic conditions). This could underestimate future (2051–2100) irrigation demand in locations with historically low levels of irrigation that are likely to expand over the next century (like many countries in Africa). Likewise, livestock water demand data ends in 2014, and is assumed to remain constant through 2100. Livestock water demand is the daily drinking water required per animal as a function of temperature (Wada et al. 2016) and amounts to less than 1 percent of global demand in 2019. Ninety-eight percent of an animal’s water footprint comes from the feed they consume (Mekonnen and Hoekstra 2012), which Aqueduct covers under irrigation demand. Still, we are underestimating future (2020–2100) livestock demand.

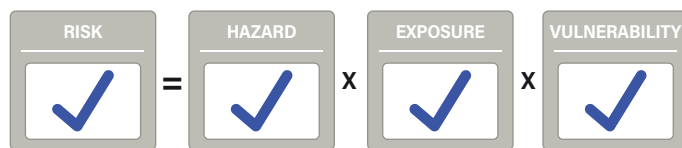
INDICATORS

For each of the 13 indicators in our framework, this section offers a description, a calculation of raw values, and a conversion to 0–5 scores. This enables us to aggregate the indicators into groups, as well as to provide an overall water risk score. For each indicator, we also include the key limitations.

Aqueduct 4.0 uses the United Nations Office for Disaster Risk Reduction (UNDRR) risk element terminology of hazard, exposure, and vulnerability. Each indicator is assigned a risk element (see Figure 5):

- **HAZARD:** Threatening event or condition (e.g., flood event, water stress condition).
- **EXPOSURE:** Elements present in the area affected by the hazard (e.g., population, asset, economic value).
- **VULNERABILITY:** The resilience or lack of resilience of the elements exposed to the hazard.

Figure 5 | Elements of risk



Source: Raw data from UNDRR, modified/aggregated by WRI.

Baseline water stress

GENERAL:	
Name	Baseline Water Stress
Subgroup	Physical risk quantity
Risk Element	$R = H \times E \times V$
RESULTS:	
Spatial resolution	Hydrological sub-basin (HydroBASINS 6)
Temporal resolution	Monthly and annual
SOURCE:	
Spatial resolution	5 x 5 arc minute grid cells
Temporal resolution	Monthly
Temporal range	1979–2019
EXTRA:	
Partner organization(s):	Utrecht University
Model	PCR-GLOBWB 2
Date of publication	2023

Description

Baseline water stress measures the ratio of total water **demand** to available renewable surface and groundwater supplies. Water demand includes domestic, industrial, irrigation, and livestock consumptive and nonconsumptive uses. Available renewable water supplies include the impact of upstream consumptive water users and large dams on downstream water availability. **Higher values indicate more competition among users.**

Calculation

Baseline water stress is calculated using the postprocessed gross demand and available blue water per sub-basin time series from the default PCR-GLOBWB 2 run (covered in “Hydrological model”).

STEP 1: CALCULATE MONTHLY WATER STRESS

$$ws_{m,b} = \max\left(1, \min\left(0, \frac{ww_{m,b}}{ba_{m,b}}\right)\right)$$

In which,

$ws_{m,b}$ = Water stress per month, per sub-basin in [-]

$ww_{m,b}$ = Total gross demand per month, per sub-basin in [million m³/month]

$ba_{m,b}$ = Available blue water per month, per sub-basin in [million m³/month]

This results in 12 time series of water stress (one for each month) per sub-basin. Additionally, we limit the raw values to a maximum of 1 and a minimum of 0. Note that water resources in delta sub-basins are pooled.

STEP 2: CALCULATE ANNUAL WATER STRESS

We calculate the annual water stress by applying a weighted average of monthly values, with total demand as the weight; months with higher demand will have more influence on the annual stress value. Months with more demand reflect when the human need for water is greatest—it is also when socioeconomic dependency for water is most critical (Gassert et al. 2013). The annual raw value ($ws_{y,b}$) is found by multiplying the monthly raw value ($ws_{m,b}$) by the monthly weight ($ww_{m,b}$), summing, and dividing by the sum of the weights across the year (y).

$$ws_{y,b} = \frac{\sum_{m=1}^{12} ww_{m,b} ws_{m,b}}{ww_{y,b}}$$

Sub-basins classified as “arid and low water use” are handled separately.

Conversion to risk categories

The risk thresholds are based on Aqueduct 2.1 (Gassert et al. 2014).

RAW VALUE	RISK CATEGORY	SCORE
<10%	Low	0-1
10–20%	Low-medium	1-2
20–40%	Medium-high	2-3
40–80%	High	3-4
>80%	Extremely high	4-5
	Arid and low water use	5

The raw values are remapped to a 0–5 scale using the following equation:

$$score = \max \left(0, \min \left(5, \frac{\ln(r) - \ln(0.1)}{\ln(2)} + 1 \right) \right)$$

Where r is the raw indicator value and score is the indicator $score [0-5]$.

Limitations

All limitations of the underlying data, including those produced by the PCR-GLOBWB 2 global hydrological model and HydroBASINS 6 hydrological sub-basin delineation, apply to this indicator. Please see the original publications of these data sets for a full list of limitations.

One of the biggest assumptions is that water resources are pooled within each sub-basin. However, in HydroBASINS 6, coastal and island sub-basins are often grouped to make the area of the sub-basins more homogeneous. The assumption of shared water resources might not hold in aggregated coastal sub-basins.

Although the underlying models have been validated, the results are not. Water stress remains subjective and cannot be measured directly. The lack of direct validation makes it impossible to assess some of the parameters in our calculation, such as the length of the input time series, regression method, and optimal moving window size.

The water stress indicator presented here does not explicitly take into account environmental flow requirements,²⁴ water quality, or access to water. Views differ regarding what to include in a water stress indicator (Vanhamb et al. 2018).

Finally, we should stress that Aqueduct is tailored to large-scale comparison of water-related risks. The indicators have limited added value on a local scale.

Baseline water depletion

GENERAL:	
Name	Baseline Water Depletion
Subgroup	Physical risk quantity
Risk Element	$R = H \times E \times V$
RESULTS:	
Spatial resolution	Hydrological sub-basin (HydroBASINS 6)
Temporal resolution	Monthly and annual
SOURCE:	
Spatial resolution	5 x 5 arc minute grid cells
Temporal resolution	Monthly
Temporal range	1979–2019
EXTRA:	
Partner organization(s):	Utrecht University
Model	PCR-GLOBWB 2
Date of publication	2023

Description

Baseline water depletion measures the ratio of total water **consumption** to available blue water. Total water consumption includes domestic, industrial, irrigation, and livestock consumptive uses. Available renewable water supplies include the impact of upstream consumptive water users and large dams on downstream water availability. **Higher values indicate larger impact on the local water supply and decreased water availability for downstream users.**

Baseline water depletion is similar to baseline water stress; however, instead of looking at gross water demand (consumptive plus nonconsumptive), baseline water depletion is calculated using consumptive withdrawal only.

Calculation

Baseline water depletion is calculated using the processed total net consumption and available blue water per sub-basin time series from the default PCR-GLOBWB 2 run (covered in “Hydrological model”).

STEP 1: CALCULATE MONTHLY WATER DEPLETION

$$wd_{m,b} = \max\left(1, \min\left(0, \frac{wn_{m,b}}{ba_{m,b}}\right)\right)$$

In which,

$wd_{m,b}$ = Water depletion per month, per sub-basin in [-]

$wn_{m,b}$ = Total net consumption per month, per sub-basin in [million m³/month]

$ba_{m,b}$ = Available blue water per month, per sub-basin in [million m³/month]

This results in 12 time series of water depletion (one for each month) per sub-basin. Additionally, we limit the raw values to a maximum of 1 and a minimum of 0. Note that water resources in delta sub-basins are pooled.

STEP 2: CALCULATE ANNUAL WATER DEPLETION

We calculate the annual water depletion by applying a weighted average of monthly values, with total net consumption as the weight; months with higher consumption will have more influence on the annual depletion value. Months with more consumption reflect when the human need for water is greatest—it is also when socioeconomic dependency for water is most critical (Gassert et al. 2013). The annual raw value ($wd_{y,b}$) is found by multiplying the monthly raw value ($wd_{m,b}$) by the monthly weight ($wn_{m,b}$), summing, and dividing by the sum of the weights across the year (y).

$$wd_{y,b} = \frac{\sum_{m=1}^{12} wn_{m,b} wd_{m,b}}{wn_{y,b}}$$

Sub-basins classified as “arid and low water use” are handled separately.

Conversion to risk categories

The thresholds are based on Brauman et al. (2016).

RAW VALUE	RISK CATEGORY	SCORE
<5%	Low	0-1
5-25%	Low-medium	1-2
25-50%	Medium-high	2-3
50-75%	High	3-4
>75%	Extremely high	4-5
Arid and low water use		5

We use linear interpolation within each category to remap the raw values to a 0–5 scale using the following equation:

$$score = \begin{cases} \max(20r, 0), r < 0.05 \\ 5r + \frac{3}{4}, 0.05 \leq r < 0.25 \\ \min(5, 4r + 1), r \geq 0.25 \end{cases}$$

Where r is the raw indicator value and $score$ is the indicator score [0–5].

Limitations

See Baseline Water Stress, Limitations (above in this section).

In addition, we had to omit the categories “dry year” and “seasonal” from Brauman et al. (2016) to make the indicator suitable for the Aqueduct framework.

Interannual variability

GENERAL:	
Name	Interannual Variability
Subgroup	Physical risk quantity
Risk Element	$R = H \times E \times V$
RESULTS:	
Spatial resolution	Hydrological sub-basin (HydroBASINS 6)
Temporal resolution	Monthly and annual
SOURCE:	
Spatial resolution	5 x 5 arc minute grid cells
Temporal resolution	Monthly
Temporal range	1979–2019
EXTRA:	
Partner organization(s):	Utrecht University
Model	PCR-GLOBWB 2
Date of publication	2023

Description

Interannual variability measures the average between-year variability of available water supply, including both renewable surface and groundwater supplies. **Higher values indicate wider variations in available supply from year to year.**

Calculation

Interannual variability is calculated using the available water time series from the default PCR-GLOBWB 2 aggregated in space but not in time. See “Hydrological model.”

Interannual, or between year, variability is defined as the coefficient of variation (CV) of available water for each sub-basin. The CV is the standard deviation (SD) of the available water, divided by the mean. The CV per sub-basin is determined for each individual month, as well as annually.

$$iav_{m,b} = cv_{m,b} = \frac{SD_{1979-2019}(ba_{m,b})}{mean_{1979-2019}(ba_{m,b})}$$

In which,

$iav_{m,b}$ = Interannual variability per month, per sub-basin in [-]

$cv_{m,b}$ = Coefficient of variation per month, per sub-basin in [-]

$ba_{m,b}$ = Available blue water per month, per sub-basin in [million m³/year]

Conversion to risk categories

The risk thresholds are based on Aqueduct 2.1 (Gassert et al. 2014).

RAW VALUE	RISK CATEGORY	SCORE
<0.25%	Low	0-1
0.25–0.50%	Low-medium	1-2
0.50–0.75%	Medium-high	2-3
0.75–1.00%	High	3-4
>1.00%	Extremely high	4-5

The raw values are remapped to a 0–5 scale using the following equation:

$$score = max(0, min(5, 4r))$$

Where r is the raw indicator value and $score$ is the indicator score [0–5].

Limitations

See Baseline Water Stress, Limitations (in this section).

In addition, we have analyzed the full time series of PCR-GLOBWB 2; that is, 1979 to 2019. We have not analyzed the effect of using a different range.

Seasonal variability

GENERAL:	
Name	Seasonal Variability
Subgroup	Physical risk quantity
Risk Element	$R = H \times E \times V$
RESULTS:	
Spatial resolution	Hydrological sub-basin (HydroBASINS 6)
Temporal resolution	Annual baseline
SOURCE:	
Spatial resolution	5 x 5 arc minute grid cells
Temporal resolution	Monthly
Temporal range	1979–2019
EXTRA:	
Partner organization(s):	Utrecht University
Model	PCR-GLOBWB 2
Date of publication	2023

Description

Seasonal variability measures the average within-year variability of available water supply, including both renewable surface and groundwater supplies. **Higher values indicate wider variations of available supply within a year.**

Calculation

Seasonal variability is calculated using the available water time series from the default PCR-GLOBWB aggregated in space but not in time. See “Hydrological model.”

First, the available water per month, per sub-basin, is calculated over the entire time series 1979–2019 (40 years).

$$\overline{ba}_{m,b} = \frac{1}{40} \sum_{y=1979}^{2019} ba_{y,m,b}, m \in \{jan \dots dec\}$$

In which,

$ba_{m,b}$ = Average available blue water per month, per sub-basin in [million m³/year]

$ba_{y,m,b}$ = Available blue water per year month, per sub-basin in [million m³/year]

The coefficient of variation is calculated using these 12 averages.

$$sev_b = \frac{SD_{[Jan \dots Dec]}(ba_{m,b})}{mean_{[Jan \dots Dec]}(\overline{ba}_{m,b})}$$

In which,

sev_b = Seasonal variability per sub-basin in [-]

$ba_{m,b}$ = Available water per month, per sub-basin in [m/month]

Conversion to risk categories

The risk thresholds are based on Aqueduct 2.1 (Gassert et al. 2014).

RAW VALUE	RISK CATEGORY	SCORE
<0.33	Low	0-1
0.33–0.66	Low-medium	1-2
0.66–1.00	Medium-high	2-3
1.00–1.33	High	3-4
>1.33	Extremely high	4-5

The raw values are remapped to a 0–5 scale using the following equation:

$$score = max(0, min(5, 3r))$$

Where r is the raw indicator value and $score$ is the indicator score [0–5].

Limitations

See Baseline Water Stress, Limitations (in this section).

Additionally, the effect of using different lengths of the input time series is not examined. The human and climatic influence on available water is likely to be more profound in recent years.

Groundwater table decline

GENERAL:	
Name	Groundwater Table Decline
Subgroup	Physical risk quantity
Risk Element	$R = H \times E \times V$
RESULTS:	
Spatial resolution	Groundwater aquifer (WHYMAP)
Temporal resolution	Annual baseline
SOURCE:	
Spatial resolution	5 x 5 arc minute grid cells
Temporal resolution	Monthly
Temporal range	1960–2014
EXTRA:	
Partner organization(s):	Deltares, Utrecht University
Model	PCR-GLOBWB 2 + MODFLOW
Date of publication	2019

Description

Groundwater table decline measures the average decline of the groundwater table as the average change for the period of study (1990–2014). The result is expressed in centimeters per year (cm/yr). **Higher values indicate higher levels of unsustainable groundwater withdrawals.**

Calculation

Groundwater table decline is calculated using the groundwater heads time series from the PCR-GLOBWB 2 run coupled with MODFLOW to account for lateral groundwater flow processes. This indicator is based on the gridded²⁵ monthly groundwater heads between January 1990 and December 2014.²⁶

The groundwater aquifers contain several geomorphological features, which for practical reasons can be divided into sedimentary basins and mountain ranges. In mountainous areas, most materials are hard rock and eventually weathered. In the PCR-GLOBWB 2 model coupled with MODFLOW, very deep groundwater influences the averages in mountainous cells and is not representative. These cells are therefore discarded from the calculations following the method in de Graaf et al. (2015).

Mountainous areas are determined by comparing the height of the floodplain within a cell with the average elevation of that same cell. The elevation of the floodplain is derived from the 30 × 30 arc second digital elevation data from HydroSheds (Lehner et al. 2008). The flood plain elevation is simply the minimum of the input.

$$h_{floodplain,5'} = \min(h_{DEM\ 30''})$$

In which,

$$h_{floodplain,5'} = \text{Elevation of floodplain in meters for each } 5 \times 5 \text{ arc minute cell}$$

$$h_{DEM\ 30''} = \text{Elevation derived from } 30 \times 30 \text{ arc second digital elevation model (DEM) in meters}$$

The average elevation for each 5 arc minute cell is taken directly from the HydroSheds data. If the difference between the floodplain elevation and the average elevation is greater than 50m, the cell is classified as mountainous.

$$\text{mountainous} = \begin{cases} \text{True, if } (h_{DEM\ 5'} - h_{floodplain,5'}) > 50m \\ \text{False, otherwise} \end{cases}$$

In which,

$$h_{floodplain,5'} = \text{Elevation of floodplain in meters for each } 5 \times 5 \text{ arc minute cell}$$

$$h_{DEM\ 5'} = \text{Elevation derived from } 5 \times 5 \text{ arc minute DEM in meters (approximately 11km at the equator)}$$

The threshold of 50m was chosen as it proved to include 70 percent of the unconsolidated sediments mapped in the Global Lithological Map (Hartmann and Moosdorf 2012).

After masking the mountainous areas, results are aggregated to groundwater aquifers derived from the Worldwide Hydrogeological Mapping and Assessment Programme (WHYMAP) data set (BGR and UNESCO 2018).

The monthly results at the aquifer scale are fitted with a first-order regression. The slope of this regression line (cm/yr) indicates the existence of a downward (or upward) trend. The following estimators are used to further assess the trend: (1) coefficient of determination and (2) the *p value*.

The coefficient of determination is used to determine whether the trend is linear or erratic. A minimum threshold of 0.9 is applied to mask out erratic and error-prone trends.

For the *p* value, a maximum threshold of 0.05 is used.

$$valid = \begin{cases} True, & \text{if } R^2 \geq 0.9 \text{ and } p \leq 0.05 \\ False, & \text{otherwise} \end{cases}$$

Conversion to risk categories

The risk category thresholds are based on a combination of expert judgment and a literature review (Galvis Rodríguez et al. 2017).

RAW VALUE	RISK CATEGORY	SCORE
<0 cm/y	Low	0-1
0-2 cm/y	Low-medium	1-2
2-4 cm/y	Medium-high	2-3
4-8 cm/y	High	3-4
>8 cm/y	Extremely high	4-5

Within each category, we use linear interpolation to convert the raw values to a 0–5 using the following equation:

$$score = \begin{cases} \max(r + 1.0), & r < 0 \\ r + 1, & 0 \leq r < 2 \\ 0.5r + 1, & 2 \leq r < 8 \\ \min(5, 0.5r + 1), & r \geq 8 \end{cases}$$

Where *r* is the raw indicator value and *score* is the indicator score [0–5].

Limitations

The limitations of PCR-GLOBWB 2, MODFLOW, WHYMAP, climate forcing, and other input data sets are propagated to these results. The results are only validated using a literature review of selected aquifers and by comparing the results to coarse remote-sensing data.

The threshold for masking out mountainous areas was set once without a sensitivity analysis. The temporal range [1990–2014] was selected on the basis of expert judgment and differs from some of the other water quantity indicators that use [1960–2014] as the input time series.

See Galvis Rodríguez et al. (2017) for additional limitations.

Riverine flood risk

GENERAL:	
Name	Riverine Flood Risk
Subgroup	Physical risk quantity
Risk Element	$R = H \times E \times V$
RESULTS:	
Spatial resolution	Hydrological sub-basin (HydroBASINS 6)
Temporal resolution	Annual baseline
SOURCE:	
Spatial resolution	30 x 30 arc minute grid cells
Temporal resolution	Annual
Temporal range	2010
EXTRA:	
Partner organization(s):	Deltares, IVM, PBL, Utrecht University
Model	GLOFRIS (Ward et al. 2020)
Date of publication	2019
Additional data source	Existing flood protection levels
Input spatial resolution	State
Input temporal resolution	Annual
Input temporal range	2016
Source	FLOPROS (Scussolini et al. 2016)

Description

Riverine flood risk measures the percentage of population expected to be affected by riverine flooding in an average year, accounting for existing flood-protection standards. Flood risk is assessed using hazard (inundation caused by river overflow), exposure (population in flood zone), and vulnerability.²⁷ The existing level of flood protection is also incorporated into the risk calculation. It is important to note that this indicator represents flood risk not in terms of maximum possible impact but rather as average annual impact. The impacts from infrequent, extreme flood years are averaged with more common, less newsworthy flood years to produce the “expected annual affected population.” **Higher values indicate that a greater proportion of the population is expected to be impacted by riverine floods on average.**

Calculation

Data on the population impacted by riverine floods are provided by Aqueduct Floods at the state/HydroBASIN 6 intersect scale (Ward et al. 2020). The data set estimates the average number of people to be impacted annually for several flood event magnitudes (2, 5, 10, 25, 50, 100, 250, 500, and 1,000 in return periods).

The *expected annual affected population* is calculated using a risk curve (Meyer et al. 2009). To create the curve, the return periods are first converted into probabilities (i.e., 1/return period) and then plotted on the *x* axis against the impacted population (Figure 6). Next, flood protection is added to the graph. The current level of flood protection, given in return years, comes from the Flood Protection Standards (FLOPROS) model (Scussolini et al. 2016). All impacts that fall to the right of the flood protection line (i.e., impacted by smaller floods) are assumed to be protected against floods and are removed from the calculation. The *expected annual affected population* is calculated by integrating the area under the curve *to the left* of the flood protection line.

The *expected annual affected population* is calculated for each state/HydroBASIN 6 intersect, then aggregated up to the HydroBASIN 6 scale. The *total population* in each state/HydroBASIN 6 intersect is also summed to the HydroBASIN 6 scale (Ward et al. 2020). Finally, the raw riverine flood risk score—the *percentage of population expected to be affected annually by riverine floods* per HydroBASIN 6—is calculated:

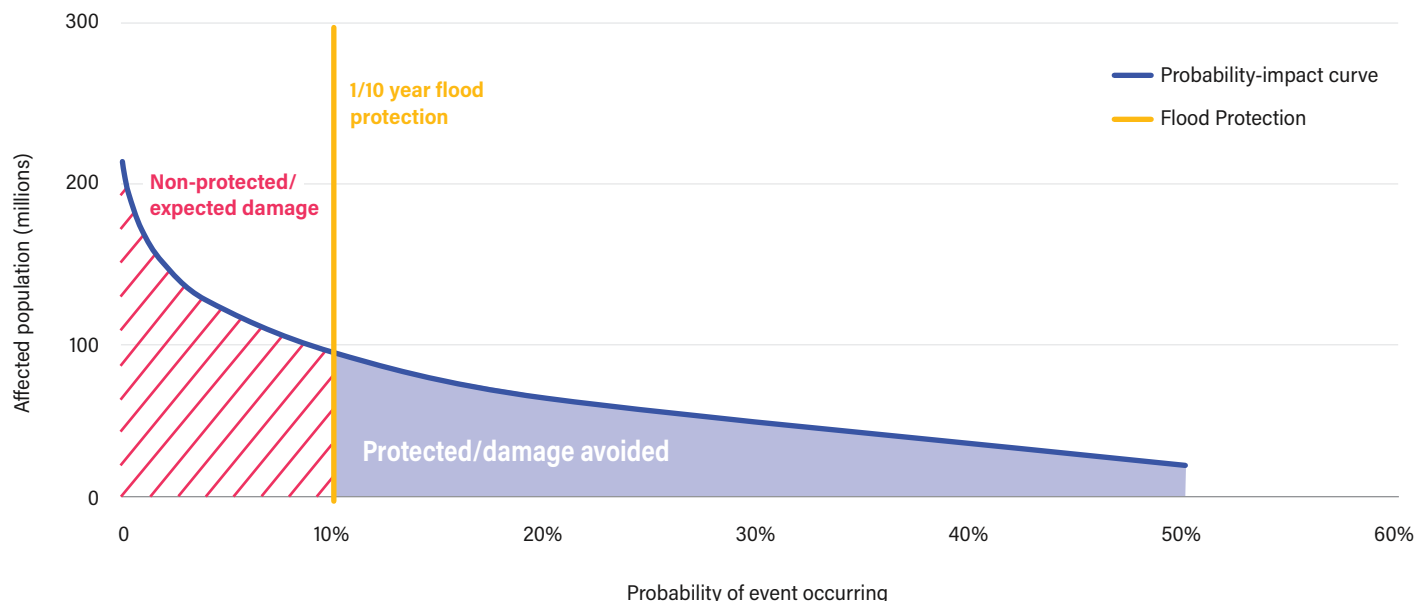
$$rfr = \frac{pop_{exp,y}}{pop_{tot}}$$

In which,

rfr = Riverine flood risk raw values in [-]

pop_{exp,y} = Expected annual affected population by riverine flooding in [number of people]

Figure 6 | Risk Curve Used to Calculate Expected Annual Affected Population from Floods



Source: WRI.

Conversion to risk categories

The thresholds are based on quantiles, with the exception of the basins with no riverine hazard. Basins without a flood hazard are given the lowest risk score, 0, and are removed from the rest of the data set before the quantiles are calculated.

RAW VALUE	RISK CATEGORY	SCORE
0 to 1 in 1,000	Low	0-1
1 in 1,000 to 2 in 1,000	Low-medium	1-2
2 in 1,000 to 6 in 1,000	Medium-high	2-3
6 in 1,000 to 1 in 100	High	3-4
More than 1 in 100	Extremely high	4-5

The raw values are remapped to a 0–5 scale using the following equation:

$$score = \begin{cases} \frac{r-0}{0.12\%-0}, & r < 0.12\% \\ \frac{r-0.12\%}{0.30\%-0.12\%} + 1, & 0.12\% \leq r < 0.30\% \\ \frac{r-0.30\%}{0.62\%-0.30\%} + 2, & 0.30\% \leq r < 0.62\% \\ \frac{r-0.62\%}{1.3\%-0.62\%} + 3, & 0.62\% \leq r < 1.3\% \\ \frac{r-1.3\%}{\max(r_{all})-1.3\%} + 4, & r \geq 1.3\% \end{cases}$$

Where r is the raw indicator value and $score$ is the indicator score [0–5].

Limitations

Riverine and coastal flood risks must be evaluated and used separately, as the compound risks between river and storm surges are not modeled. The data also assume that flood events are entirely independent of each other, so the impact from overlapping flood events is not considered. Finally, the data do not include any indirect impacts from flooding (e.g., disrupted transportation, loss of work, etc.).

Coastal flood risk

GENERAL:	
Name	Coastal Flood Risk
Subgroup	Physical risk quantity
Risk Element	$R = H \times E \times V$
RESULTS:	
Spatial resolution	Hydrological sub-basin (HydroBASINS 6)
Temporal resolution	Annual baseline
SOURCE:	
Spatial resolution	30 x 30 arc minute grid cells
Temporal resolution	Annual
Temporal range	2010
EXTRA:	
Partner organization(s):	Deltares, IVM, PBL, Utrecht University
Model	GLOFRIS (Ward et al. 2020)
Date of publication	2019

Additional data source	Existing flood protection levels
Input spatial resolution	State
Input temporal resolution	Annual
Input temporal range	2016
Source	FLOPROS (Scussolini et al. 2016)

Description

Coastal flood risk measures the percentage of the population expected to be affected by coastal flooding in an average year, accounting for existing flood protection standards. Flood risk is assessed using hazard (inundation caused by storm surge), exposure (population in flood zone), and vulnerability.²⁸ The existing level of flood protection is also incorporated into the risk calculation. It is important to note that this indicator represents flood risk not in terms of maximum possible impact but rather as average annual impact. The impacts from infrequent, extreme flood years are averaged with more common, less newsworthy flood years to produce the “expected annual affected population.” **Higher values indicate that a greater proportion of the population is expected to be impacted by coastal floods on average.**

Calculation

Data on the population impacted by coastal floods are provided by Aqueduct Floods at the state/HydroBASIN 6 intersect scale (Ward et al. 2020). The data set estimates the average number of people to be impacted annually for several flood event magnitudes (2, 5, 10, 25, 50, 100, 250, 500, and 1,000 in return periods).

The *expected annual affected population* is calculated using a risk curve (Meyer et al. 2009). To create the curve, the return periods are first converted into probabilities (i.e., 1/return period) and then plotted on the *x* axis against the impacted population (Figure 6). Next, vulnerability—or flood protection—is added to the graph as a vertical line. The current level of flood protection, given in return years, comes from the FLOPROS model (Scussolini et al. 2016). All impacts that fall to the right of the flood protection line (i.e., impacted by smaller floods) are assumed to be protected against floods and are removed from the calculation. The *expected annual affected population* is calculated by integrating the area under the curve *to the left* of the flood protection line.

The *expected annual affected population* is calculated for each state/HydroBASIN 6 intersect and then aggregated up to the HydroBASIN 6 scale. The *total population* in each state/HydroBASIN 6 intersect is also summed to the HydroBASIN 6 scale (Ward et al. forthcoming). Finally, the raw coastal flood risk score—the *percentage of population expected to be affected annually by coastal floods* per HydroBASIN 6—is calculated:

$$cfr = \frac{pop_{exp,c,y}}{pop_{tot}}$$

In which,

cfr = Coastal flood risk raw values in [-]

$pop_{exp,c,y}$ = Expected annual affected population by coastal flooding in [number of people]

Conversion to risk categories

The thresholds are based on quantiles, with the exception of the basins with no coastal hazard. Basins without a flood hazard are given the lowest risk score, -1, and removed from the rest of the data set before the quantiles are calculated.

RAW VALUE	RISK CATEGORY	SCORE
0 to 9 in 1,000,000	Low	0
9 in 1,000,000 to 7 100,000	Low-medium	1-2
7 in 100,000 to 3 in 10,000	Medium-high	2-3
3 in 10,000 to 2 in 1,000	High	3-4
More than 2 in 1,000	Extremely high	4-5

The raw values are remapped to a 0–5 scale using the following equation:

$$score = \begin{cases} \frac{r-0}{0.001\%-0}, & r < 0.001\% \\ \frac{r-0.001\%}{0.007\%-0.001\%} + 1, & 0.001\% \leq r < 0.007\% \\ \frac{r-0.007\%}{0.04\%-0.007\%} + 2, & 0.007\% \leq r < 0.04\% \\ \frac{r-0.04\%}{0.22\%-0.04\%} + 3, & 0.04\% \leq r < 0.22\% \\ \frac{r-0.22\%}{\max(r_{all})-0.22\%} + 4, & r \geq 0.22\% \end{cases}$$

Where r is the raw indicator value and $score$ is the indicator score [0–5].

Limitations

Riverine and coastal flood risks must be evaluated and used separately, as the compound risks between river and storm surges are not modeled. The data also assume that flood events are entirely independent of each other, so the impact from overlapping flood events is not considered. Finally, the data do not include any indirect impacts from flooding (e.g., disrupted transportation, loss of work, etc.).

Drought risk

GENERAL:	
Name	Drought Risk
Subgroup	Physical risk quantity
Risk Element	$R = H \times E \times V$
RESULTS:	
Spatial resolution	Hydrological sub-basin (HydroBASINS 6)
Temporal resolution	Annual baseline
SOURCE:	
Spatial resolution	5 x 5 arc minute grid cells
Temporal resolution	Annual
Temporal range	2000–2014
EXTRA:	
Partner organization(s):	IRC
Model	Various
Date of publication	2016

Description

Drought risk measures where droughts are likely to occur, the population and assets exposed, and the vulnerability of the population and assets to adverse effects. **Higher values indicate higher risk of drought.**

Calculation

The drought risk indicator is based on Carrão et al. (2016) and is used with minimal alterations. Drought risk is assessed for the period 2000–2014 and is a combination of drought hazard, drought exposure, and drought vulnerability.

$$Risk = hazard \times exposure \times vulnerability$$

The methodology is explained in Carrão et al. (2016):

Drought hazard is derived from a non-parametric analysis of historical precipitation deficits at the 0.5 [degree resolution]; drought exposure is based on a non-parametric aggregation of gridded indicators of population and livestock densities, crop cover and water stress; and drought vulnerability is computed as the arithmetic composite of high level factors of social, economic and infrastructural indicators, collected at both the national and sub-national levels.

The hazard, exposure, vulnerability, risk, and no-data mask data available at 5 × 5 arc minute resolution are averaged for each hydrological sub-basin.

$$dr_{subbasin} = \frac{1}{n_{pix}} \sum_{i=1}^{n_{pix}} dr_{pix}$$

In which,

$dr_{subbasin}$ = Drought risk per sub-basin

n_{pix} = Number of pixels per sub-basin

dr_{pix} = Drought risk per pixel

Conversion to risk categories

The risk categories are derived from Carrão et al. (2016):

RAW VALUE	RISK CATEGORY	SCORE
0.0–0.2	Low	0
0.2–0.4	Low-medium	1–2
0.4–0.6	Medium	2–3
0.6–0.8	Medium-high	3–4
0.8–1.0	High	4–5

The raw values are remapped to a 0–5 scale using the following equation:

$$score = 5r$$

Where r is the raw indicator value and $score$ is the indicator score [0–5].

Limitations

Many of the indicators in the Aqueduct water risk framework represent a hazard. Some indicators, including drought risk, add exposure and vulnerability. Aqueduct combines these risk elements into a single framework.

The drought risk indicator does not consider hydrological drought and excludes associated risks such as unnavigable rivers.

Other Aqueduct risk categories are typically skewed toward the higher side, with the category “extremely high” as the top category. The drought risk indicator has not been interpreted yet and is therefore presented at a low–high scale instead of low–extremely high.

See Carrão et al. (2016) for limitations of the different risk elements (hazard, exposure, vulnerability) and the input data sets.

Untreated connected wastewater

GENERAL:	
Name	Untreated Connected Wastewater
Subgroup	Physical risk quantity
Risk Element	$R = H \times E \times V$
RESULTS:	
Spatial resolution	Country
Temporal resolution	Annual baseline
SOURCE:	
Spatial resolution	Country
Temporal resolution	Annual
Temporal range	2000–2010
EXTRA:	
Partner organization(s):	IFPRI, Veolia
Model	Various
Date of publication	2016

Description

Untreated connected wastewater measures the percentage of domestic wastewater that is connected through a sewerage system and not treated to at least a primary treatment level. Wastewater discharge without adequate treatment could expose water bodies, the general public, and ecosystems to pollutants such as pathogens and nutrients. The indicator compounds two crucial elements of wastewater management: connection and treatment. Low connection rates reflect households' lack of access to public sewerage systems; the absence of at least primary treatment reflects a country's lack of capacity (infrastructure, institutional knowledge) to treat wastewater. Together these factors can indicate the level of a country's current capacity to manage its domestic wastewater through two main pathways: extremely low connection rates (below 1 percent), and high connection rates with little treatment. **Higher values indicate higher percentages of point source wastewater discharged without treatment.**

Calculation

Sewerage connection and wastewater treatment data come from a white paper published by the International Food Policy Research Institute (IFPRI) and Veolia (Xie et al. 2016). In brief, Xie et al. aggregate three of the leading research papers

on country-level connection and treatment rates into one data set through a hierarchical methodology. The data include the percentage of households connected to sewerage systems (*percent connected*), and the percentage of wastewater connected left untreated (i.e., not treated using primary, secondary, or tertiary treatments) (*percent untreated*).

The calculation is based on the Environmental Performance Index's Wastewater Treatment (WWT) indicator (Wendling et al. 2018):

$$WWT = \text{percent treated to at least primary} * \text{percent connected}$$

WWT examines the performance of wastewater treatment (Wendling et al. 2018). The untreated, connected wastewater indicator reverses the WWT to instead examine the hazard:

$$UCW = \begin{cases} -1, & c \leq 1\% \\ 100\% - ((100\% - u) \cdot c), & \text{otherwise} \end{cases}$$

In which,

UCW = Unimproved/connected wastewater raw value in [%]

c = Percent connected wastewater in [%]

u = Percent untreated wastewater in [%]

Conversion to risk categories

The risk thresholds are based on quantiles, with the exception of the “low to no wastewater connected” threshold. All data marked in this category are given the highest risk score and removed from the rest of the data set before the quantiles are calculated.

RAW VALUE	RISK CATEGORY	SCORE
<30%	Low	0
30–60%	Low-medium	1–2
60–90%	Medium-high	2–3
90–100%	High	3–4
100%	Extremely high	4–5
	Low to no wastewater connected	5

The raw values are remapped to a 0–5 scale using the following equation:

$$score = \begin{cases} 5, & r < 0\% \\ \frac{r-0}{30\%-0}, & r \leq 30\% \\ \frac{r-30}{60\%-30} + 1, & 30\% < r \leq 60\% \\ \frac{r-60}{90\%-60} + 2, & 60\% < r \leq 90\% \\ \frac{r-90}{99\%-90} + 3, & 90\% < r < 100\% \\ 5, & r = 100\% \end{cases}$$

Where r is the raw indicator value and $score$ is the indicator score [0–5].

Limitations

Important sources of water pollution, such as industrial waste and agricultural runoff, are not included. Wastewater that may be treated on-site, such as with private septic tanks, is also not captured due to a lack of available data. In addition, the severity of water pollution, which depends on the magnitude of loadings of pollutants and dilution capacity of receiving water bodies, is not represented (from a 2017 personal communication with Xie). This indicator also does not account for all water pollution sources, as it is focused primarily on household connection rates.

Coastal eutrophication potential

GENERAL:	
Name	Coastal Eutrophication Potential
Subgroup	Physical risk quality
Risk Element	$R = H \times E \times V$
RESULTS:	
Spatial resolution	Hydrological sub-basin (HydroBASINS 6)
Temporal resolution	Annual baseline
SOURCE:	
Spatial resolution	Simulated Topological Network (STN)
Temporal resolution	Annual
Temporal range	2000
EXTRA:	
Partner organization(s):	Utrecht University, Washington State University
Model	NA
Date of publication	2016
Additional data source	STN Basins
Input spatial resolution	30 x 30 arc seconds
Input temporal resolution	Annual
Input temporal range	2000
Source	Vörösmarty et al. (2000)

Description

Coastal eutrophication potential (CEP) measures the potential for riverine loadings of nitrogen (N), phosphorus (P), and silica (Si) to stimulate harmful algal blooms in coastal waters. The CEP indicator is a useful metric to map where anthropogenic activities produce enough point-source and nonpoint-source pollution to potentially degrade the environment. When N and P are discharged in excess over Si with respect to diatoms, a major type of algae, undesirable algal species often develop. The stimulation of algae leading to large blooms may in turn result in eutrophication and hypoxia (excessive biological growth and decomposition that reduces oxygen available to other organisms). It is therefore possible to assess the potential for coastal eutrophication from a river's N, P, and Si loading. **Higher values**

indicate higher levels of excess nutrients with respect to silica, creating more favorable conditions for harmful algal growth and eutrophication in coastal waters downstream.

Calculation

The calculation described below is based on Billen and Garnier's (2007) Indicator of Coastal Eutrophication Potential (ICEP) methodology. The nutrient data come from Bouwman et al. (2015). In short, the data are based on the Global NEWS 2 model (Mayorga et al. 2010) and aligned to Simulated Topological Network basins (Vörösmarty et al. 2000). The NEWS 2 model uses biophysical, natural, and anthropogenic (both point and nonpoint) nutrient sources, along with in-watershed and in-river removal processes, to derive global nutrient yields (Mayorga et al. 2010). Total N and P fluxes are calculated by summing NEWS 2 nutrient yield data for dissolved organic, dissolved inorganic, and particulate nutrients. Si fluxes are simply the dissolved inorganic Si yields in the basin.

The calculation is based on the Redfield molar ratio (C:N:P:Si = 106:16:1:20), which is a representation of the approximate nutrient requirement of marine diatoms (Billen and Garnier 2007):

$$CEP = \begin{cases} \left(\frac{j_N}{N \cdot 16} - \frac{j_{Si}}{Si \cdot 20} \right) \cdot 106 \cdot \frac{12}{365}, & \text{if } \frac{j_N}{N \cdot 16} > \frac{j_P}{P \cdot 1} \\ \left(\frac{j_P}{P \cdot 1} - \frac{j_{Si}}{Si \cdot 20} \right) \cdot 106 \cdot \frac{12}{365}, & \text{otherwise} \end{cases}$$

In which,

CEP = Coastal eutrophication potential [kg C-equivalent km²/day]

j_N = Mean flux of total nitrogen delivered at the outlet of the river basin [kg N/km²/yr]

j_P = Mean flux of total phosphorus delivered at the outlet of the river basin [kg P/km²/yr]

j_{Si} = Mean flux of dissolved silica delivered at the outlet of the river basin [kg Si/km²/yr]

N = Molar mass of nitrogen [14g/mol]

Si = Molar mass of silica [28g/mol]

P = Molar mass of phosphorus [14g/mol]

A negative value indicates that silica is present in excess over the limiting nutrient and thus suggests the absence of eutrophication. A positive value indicates an excess of nutrients over the

potential for diatom growth, suggesting suitable conditions for the growth of harmful algae (Garnier et al. 2010).

As a final step, the results are aggregated to HydroBASIN level 6 to align the indicator with the remainder of the framework.

Conversion to risk categories

The thresholds used to convert raw values into risk scores are based on the suggested risk categories of the Transboundary Water Assessment Programme (TWAP) for ICEP (IOC-UNESCO and UNEP 2016), with one adjustment: the boundary between TWAP's low and medium categories was increased from -1 to 0 to better reflect the elevated risk warning in Aqueduct.

RAW VALUE	RISK CATEGORY	SCORE
<-5	Low	0-1
-5-0	Low-medium	1-2
0-1	Medium-high	2-3
1-5	High	3-4
>5	Extremely high	4-5

The raw values are remapped to a 0–5 scale using the following equation:

$$score = \begin{cases} \frac{r - min(r_{all})}{-5 - min(r_{all})}, & r \leq -5 \\ \frac{r - -5}{0 - -5} + 1, & -5 < r \leq 0 \\ \frac{r - 0}{1 - 0} + 2, & 0 < r \leq 1 \\ \frac{r - 1}{5 - 1} + 3, & 1 < r \leq 5 \\ \frac{r - 5}{max(r_{all}) - 5} + 4, & r > 5 \end{cases}$$

Where r is the raw indicator value and $score$ is the indicator score [0–5].

Limitations

Eutrophication can also impact freshwater, but a global data set for freshwater eutrophication potential is not currently available. Therefore, the indicator does not reflect the risk of eutrophication upstream of the coastal zone. In addition, the index calculation does not account for shifts in seasonality or the characteristics of the receiving water body.

Unimproved/No drinking water

GENERAL:	
Name	Unimproved/No Drinking Water
Subgroup	Regulatory and reputational risk
Risk Element	$R = H \times E \times V$
RESULTS:	
Spatial resolution	Hydrological sub-basin (HydroBASINS 6)
Temporal resolution	Annual baseline
SOURCE:	
Spatial resolution	Country (rural/urban)
Temporal resolution	Annual
Temporal range	2015
EXTRA:	
Partner organization(s):	JMP
Model	NA
Date of publication	2017

Additional data source	Urban extents	Gridded population
Input spatial resolution	30 arc seconds	30 arc seconds
Input temporal resolution	Annual	Annual
Input temporal range	2010	2010
Source	van Huijstee et al. (2018)	van Vuuren et al. (2007)

Description

Unimproved/no drinking water reflects the percentage of the population collecting drinking water from an unprotected dug well or spring, or directly from a river, dam, lake, pond, stream, canal, or irrigation canal (WHO and UNICEF 2017). Specifically, the indicator aligns with the *unimproved and surface water* categories of the Joint Monitoring Programme (JMP)—the lowest tiers of drinking water services. **Higher values indicate areas where people have less access to safe drinking water supplies.**

Calculation

Data for this indicator come from the 2015 drinking water access rates published by JMP (WHO and UNICEF 2017). The statistics from JMP's "at least basic" and "limited" fields

are summed to represent the percentage of the population with access to *improved* drinking water. The *improved* rate is then inverted into the *unimproved/no access* rate by subtracting *improved* from 100 percent. This is done for the national, rural, and urban averages in each country. The national average is used to fill in any missing rural or urban averages.

The *unimproved/no access* rate is matched to each Aqueduct geometry (intersect of states, HydroBASIN 6, and aquifers; see 6.1) using the International Organization for Standardization (ISO) codes provided by the Database of Global Administrative Areas (GADM) ("GADM Metadata" n.d.).

Rural and urban populations are calculated for each Aqueduct geometry. Rural and urban populations come from a gridded 2010 population data set produced by the Netherlands Environmental Assessment Agency (PBL) (van Vuuren et al. 2007). The gridded population data set is parsed into rural and urban populations using a 2010 urban extent data layer (van Huijstee et al. 2018) and then summed by Aqueduct geometry.

The rural and urban *unimproved/no access* rate is multiplied by the *rural and urban populations*, respectively, to find the *number of people with unimproved/no access* to drinking water in each Aqueduct geometry. The rural and urban totals are then summed and aggregated to the HydroBASIN 6 scale, along with *total population*. Finally, the raw score—the *weighted percentage of population with unimproved/no access* per HydroBASIN 6—is calculated:

$$UDW = \frac{\sum_{basin} (r_{rural} \cdot pop_{rural} + r_{urban} \cdot pop_{urban})}{\sum_{basin} (pop_{tot})}$$

In which,

UDW = Unimproved/no drinking water raw value in [-]

r_{rural} = Rural unimproved/no access to drinking water rate in [-]

r_{urban} = Urban unimproved/no access to drinking water rate in [-]

pop_{rural} = Rural population in [number of people]

pop_{urban} = Urban population in [number of people]

pop_{tot} = Total population in [number of people]

Conversion to risk categories

The risk thresholds are based on Aqueduct 2.1 (Gassert et al. 2014).

RAW VALUE	RISK CATEGORY	SCORE
<2.5%	Low	0-1
2.5–5.0%	Low-medium	1-2
5.0–10.0%	Medium-high	2-3
10.0–20.0%	High	3-4
>20.0%	Extremely high	4-5

The raw values are remapped to a 0–5 scale using the following equation:

$$score = \max\left(0, \min\left(\frac{\ln(r) - \ln(0.025)}{\ln(2)}\right) + 1\right)$$

Where r is the raw indicator value and $score$ is the indicator score [0–5].

Limitations

The unimproved/no drinking water indicator is presented at a finer resolution than originally published by JMP under the assumption that access rates among rural and urban communities are consistent throughout a country. The methodology fails to account for regional and local differences in access within countries.

Unimproved/No sanitation

GENERAL:	
Name	Unimproved/No Drinking Sanitation
Subgroup	Regulatory and reputational risk
Risk Element	$R = H \times E \times V$
RESULTS:	
Spatial resolution	Hydrological sub-basin (HydroBASINS 6)
Temporal resolution	Annual baseline
SOURCE:	
Spatial resolution	Country (rural/urban)
Temporal resolution	Annual
Temporal range	2015
EXTRA:	
Partner organization(s):	JMP
Model	NA
Date of publication	2017

Additional data source	Urban extents	Gridded population
Input spatial resolution	30 arc seconds	30 arc seconds
Input temporal resolution	Annual	Annual
Input temporal range	2010	2010
Source	van Huijstee et al. (2018)	van Vuuren et al. (2007)

Description

Unimproved/no sanitation reflects the percentage of the population using pit latrines without a slab or platform, hanging/bucket latrines, or directly disposing human waste in fields, forests, bushes, open bodies of water, beaches, other open spaces, or with solid waste (WHO and UNICEF 2017). Specifically, the indicator aligns with JMP's *unimproved and open defecation categories*—the lowest tier of sanitation services. **Higher values indicate areas where people have less access to improved sanitation services.**

Calculation

Data for this indicator come from the 2015 sanitation access rates published by JMP (WHO and UNICEF 2017). Statistics from JMP's “at least basic” and “limited” fields are summed to represent the percentage of the population with access to improved sanitation. The improved rate is then inverted into the unimproved/no access rate by subtracting improved from 100 percent. This is done for the national, rural, and urban averages in each country. The national average is used to fill in any missing rural or urban averages.

The unimproved/no access rate is matched to each Aqueduct geometry (intersect of states, HydroBASINS 6, and aquifers; see 6.1) using the International Organization for Standardization (ISO) codes provided by GADM (“GADM Metadata” n.d.).

Rural and urban populations are calculated for each Aqueduct geometry. Rural and urban populations come from a gridded 2010 population data set produced by PBL (van Vuuren et al. 2007). The gridded population data set is parsed into rural and urban populations using a 2010 urban extent data layer (van Huijstee et al. 2018), and then summed by Aqueduct geometry.

The rural and urban *unimproved/no access rate* is multiplied by the *rural and urban populations*, respectively, to find the number of people with *unimproved/no access* to sanitation in each Aqueduct geometry. The rural and urban totals are then summed and aggregated to the HydroBASINS 6 scale, along with *total population*. Finally, the raw score—the *weighted percentage of population with unimproved/no access* per HydroBASINS 6—is calculated:

$$USA = \frac{\sum_{basin} (r_{rural} \cdot pop_{rural} + r_{urban} \cdot pop_{urban})}{\sum_{basin} (pop_{tot})}$$

In which,

USA = Unimproved/no sanitation raw value in [-]

r_{rural} = Rural unimproved/no access to sanitation rate in [-]

r_{urban} = Urban unimproved/no access to drinking water rate in [-]

pop_{rural} = Rural population in [number of people]

pop_{urban} = Urban population in [number of people]

pop_{tot} = Total population in [number of people]

Conversion to risk categories

The risk thresholds are based on Aqueduct 2.1 (Gassert et al. 2014).

RAW VALUE	RISK CATEGORY	SCORE
<2.5%	Low	0-1
2.5–5.0%	Low-medium	1-2
5.0–10.0%	Medium-high	2-3
10.0–20.0%	High	3-4
>20.0%	Extremely high	4-5

The raw values are remapped to a 0–5 scale using the following equation:

$$score = \max\left(0, \min\left(\frac{\ln(r) - \ln(0.025)}{\ln(2)}\right) + 1\right)$$

Where r is the raw indicator value and $score$ is the indicator score [0–5].

Limitations

Unimproved/no sanitation is presented at a finer resolution than is originally published by JMP under the assumption that access rates among rural and urban communities are consistent throughout a country. The methodology fails to account for regional and local differences in access within countries.

Peak RepRisk country ESG risk index

GENERAL:	
Name	Peak RepRisk Country EDG Risk Index
Subgroup	Regulatory and reputational risk
Risk Element	$R = H \times E \times V$
RESULTS:	
Spatial resolution	Country
Temporal resolution	Annual baseline
SOURCE:	
Spatial resolution	Country
Temporal resolution	Annual
Temporal range	2016–2018
EXTRA:	
Partner organization(s):	RepRisk
Model	NA
Date of publication	2018

Description

The Peak RepRisk country ESG risk index quantifies business conduct risk exposure related to environmental, social, and governance (ESG) issues in the corresponding country. The index provides insights into potential financial, reputational, and compliance risks, such as human rights violations and environmental destruction. RepRisk is a leading business intelligence provider that specializes in ESG and business conduct risk research for companies, projects, sectors, countries, ESG issues, NGOs, and more, by leveraging artificial intelligence and human analysis in 20 languages. WRI has elected to include the Peak RepRisk country ESG risk index in Aqueduct to reflect the broader regulatory and reputational risks that may threaten water quantity, quality, and access. While the underlying algorithm is proprietary, we believe that our inclusion of the Peak RepRisk country ESG risk index, normally unavailable to the public, is a value-add to the Aqueduct community. The peak value equals the highest level of the index in a given country over the last two years. **The higher the value, the higher the risk exposure.**

Calculation

RepRisk screens over 80,000 media, stakeholder, and third-party sources daily to identify and analyze ESG-related risk incidents and quantify them into the Peak RepRisk country ESG risk

index (RepRisk n.d.). The results of the screening process are delivered to the RepRisk team of analysts, who are responsible for curating and analyzing the information. They hand select the items, give each risk incident a score (based on severity, source, and novelty), and write a risk summary. Before the risk incident is published, a senior analyst runs a quality check to ensure that the process has been completed in line with RepRisk's strict, rules-based methodology. After the senior analyst has given her or his approval, the final step in the process, the quantification of the risk, is performed through data science. The Peak RepRisk country ESG risk index takes into consideration the impact of a country's risk incidents within the last two years and the average of a country's Worldwide Governance Indicators. The data used in Aqueduct 3.0 cover October 2016 through October 2018. To learn more about RepRisk, please visit <https://www.reprisk.com/our-approach> or contact RepRisk.

Conversion to risk categories

The risk thresholds are based on guidance from RepRisk (RepRisk n.d.).

RAW VALUE	RISK CATEGORY	SCORE
<25%	Low	0-1
25–50%	Low-medium	1-2
50–60%	Medium-high	2-3
60–75%	High	3-4
>75%	Extremely high	4-5

The raw values are remapped to a 0–5 scale using the following equation:

$$score = \begin{cases} \frac{r}{25\%}, & r \leq 25\% \\ \frac{r-25\%}{50\%-25\%} + 1, & 25\% < r \leq 50\% \\ \frac{r-50\%}{60\%-50\%} + 2, & 50\% < r \leq 60\% \\ \frac{r-60\%}{75\%-60\%} + 3, & 60\% < r \leq 75\% \\ \frac{r-75\%}{100\%-75\%} + 4, & r > 75\% \end{cases}$$

Where r is the raw indicator value and $score$ is the indicator score [0–5].

COUNTRY AND STATE AGGREGATION

The updated country and state aggregations of the baseline and future projection data follow the weighted aggregation methodology published in Gassert et al. 2013. We provide an excerpt of their rationale and methods here for your convenience:

Most water-related decisions are made across political or administrative boundaries, creating a demand for simple and robust water information to support decision making at the administrative level. Governments devise policies to manage water resources within their borders and can use country indicators as a statistic against which to benchmark themselves. Many financial institutions divide their portfolios by country, and thus require national-level water data to evaluate portfolio exposure to water-related risks.

However, accurately assessing the state of water resources across administrative boundaries is a significant challenge; and simple, comparable, and robust water information to support decision making at that level remains sparse. The spatial variation of water resources complicates the development of meaningful country and basin-level indicators. As opposed to other resources such as forests and agricultural lands, whose stationarity simplifies measurement and management, water cannot be accounted for by using only administrative boundaries. Even within small administrative regions, hydrological conditions may vary from lush rainforest to dry prairie. Transboundary lakes and rivers further complicate water accounting, as special efforts must be made to avoid double counting the water supply, they provide across regions.

The Aqueduct Water Risk Atlas (Aqueduct) first models global water-risk indicators at a relatively granular hydrological catchment scale. In this analysis WRI then employs a weighted aggregation methodology that brings Aqueduct's catchment-level information up to the country and state levels. This methodology addresses each of the challenges described above by starting with indicators that were computed within basic hydrological units, and assigning spatially explicit weights to reflect the importance of the specific areas based on where water is being used. From these calculations, WRI generated estimates of the average level of exposure to Aqueduct's baseline water stress indicator for all countries.

Inputs

This section details the methodology to aggregate Aqueduct indicators from the sub-basin level to state and country borders. The methodology requires three inputs: gridded weights to define where water is being used, an Aqueduct indicator score to rescale, and target regions (state and country borders).

Gridded weights

The gross demand data is used to indicate where human need for water is greatest—it is also where socioeconomic dependency for water is most critical (Gassert et al. 2013). Areas with higher water demand will have more influence over the final aggregated score. We use the following gridded demand data sets from PCR-GLOBWB 2:

Baseline gross demand for four sectors: domestic, industrial, irrigation, and livestock. The 4 gridded data sets are available for each month between January 1960 and December 2019.

Projected gross demand for four sectors—domestic, industrial, irrigation, and livestock—available for each month between January 1960 and December 2100. Domestic, industrial, and livestock demand vary among the three future scenarios, meaning there are 3 data sets per demand type for every time step. Irrigation²⁹ also varies by GCM (5 total) within each scenario, meaning there are (5 x 3=) 15 irrigation data sets available for every time step. See “Future projections” for more details on the future projections data.

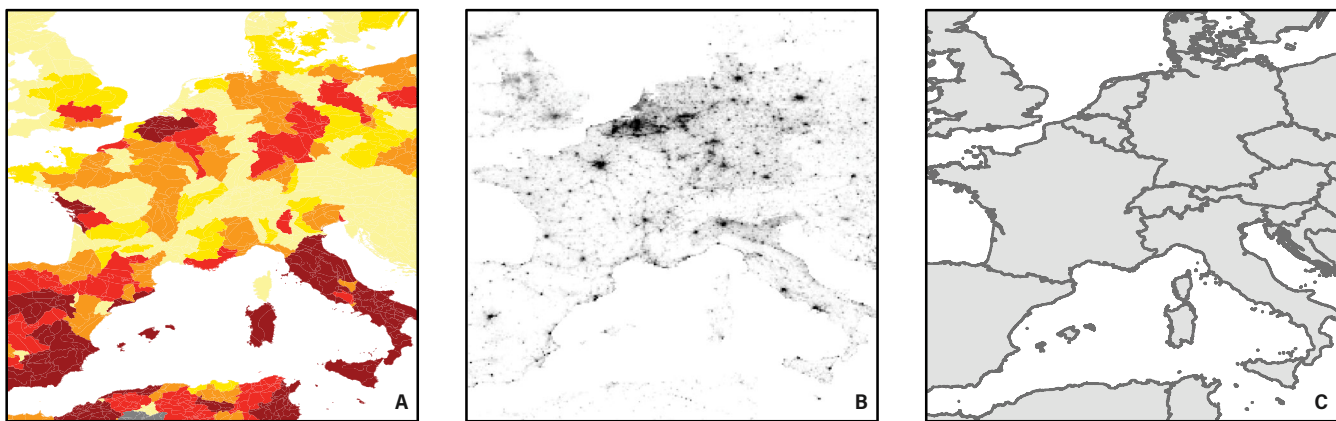
Aqueduct indicators

Water stress measures the competition over water resources and is an effective metric to evaluate water-related risks at the state and country levels. We take the water stress score—the normalized version of the raw data—for the baseline, 2030, 2050, and 2080. See the first section of “Indicators” for more details on how the water stress score is calculated.

Target regions

Our target geometries are state and country borders. We use GADM Level 1 data (GADM Metadata n.d.) to define the borders. These are state borders, which inherently also contain country borders. We intersect the GADM Level 1 data with the HydroBASIN level 6 data (sub-basins used by Aqueduct) to traverse between the two systems.

Figure 7 | Examples of the Three Spatially Explicit Inputs



Notes: a. Source indicators: baseline water stress; b. Gridded weights: total water withdrawal; c. Target regions: country boundaries.

Source: WRI Aqueduct.

Weighted aggregation

Processing gridded weights

First, we sum the gridded gross demand monthly layers into annual data. Then, we follow the same methodology described in the *Spatial aggregation of water use* section (in 2.3.1)—we resample, convert flux to volume, and sum per target geometry. The only difference is we use the state/sub-basin intersect as the target geometry rather than the sub-basins. Next, we then summarize the data by the following milestone years:

- Baseline: 1979–2019 (historic observed climate forcing)
- 2014: 1960–2014 (historic GCM climate forcing)
- 2030: 2015–2045 (future GCM climate forcing)
- 2050: 2035–2065 (future GCM climate forcing)
- 2080: 2065–2095 (future GCM climate forcing)

To do this, we follow the *Temporal Aggregation* steps outlined in “Hydrological model”—we calculate total demand by summing sectoral demand, smooth the data using a 10-year moving average, and apply a Theil Sen regression—with two exceptions: (1) we do not split the data by months because we are only using annual data, and (2) we perform the temporal aggregation of the individual sectors as well as total demand. Finally, we bias-correct the projected demand data to the baseline using the methodology outlined in “Future projections.” For the projected demand, we use the median value of the five GCMs to represent each scenario.

In the end, we have five measures of gross demand (total, domestic, industrial, irrigation, livestock) for five time periods (baseline, 2014, 2030, 2050, and 2080) for the three SSP scenarios (for the future periods).

Applying the weighted average

We compute the average water stress score for every target region (i.e., states and countries) using a weighted average approach, where the weight is water demand. Following Gassert et al. 2013, the weighted mean indicator value (s_r) is found by multiplying the sub-basin indicator (s_p) by the state-sub-basin weight (w_p), summing, and dividing by the sum of the weights across the entire administrative region (r).

$$s_r = \frac{\sum_{p \in r} w_p s_p}{\sum_{p \in r} w_p}$$

GROUPED AND OVERALL WATER RISK

After calculating the 13 indicators and converting them to a uniform 0–5 scale, we can calculate the grouped and overall water risks (composite indices). See Figure 1 for an overview of the groups.

Geometries

Each of the 13 indicators is calculated at one of three different spatial scales: hydrological sub-basin, country, or groundwater aquifer. See “results: spatial resolution” in the summary table of each indicator. To combine the indicators into one framework, we take the union of the three geometries. The resulting geometries are a unique combination of a hydrological basin, groundwater aquifers, and an administrative boundary.

Weighted aggregation

The subgroups (physical risk quantity, physical risk quality, and regulatory and reputational risk) and overall risks are calculated by taking a weighted average of the indicators that belong to each subgroup.

Exposure to water-related risks varies with the characteristics of water users. To obtain aggregated water risk scores, users can modify the weight of each indicator to match their exposure to the different aspects of water risk. There are five weights, or descriptors of relevance, on a base 2 exponential scale. This is preferred over a linear scale because of the human tendency to categorize intensity by orders of magnitude of difference (Triantaphyllou 2010). Users can also exclude indicators completely from aggregation. See Table 2 for an overview of the weights.

Users have three options for the weighting scheme: default, industry-specific, or custom.

Default weighting scheme

To determine a default set of indicator weights, we used input from six staff water experts following the principles of the Delphi technique. This technique uses a series of intensive questionnaires interspersed with controlled opinion feedback to obtain the most reliable consensus of opinion from a group of experts (Rowe and Wright 1999). The Delphi technique is intended for use in judgment situations; that is, ones in which pure model-based statistical methods are not practical or possible because of the lack of appropriate historical data, and thus some form of human judgment input is necessary (Dalkey and Helmer 1963). The lack of consistent information on exposure

Table 2 | Industry or user relevance weights and their descriptions

LEGEND	WEIGHT	INTERPRETATION
No weight	0	Not relevant
Very low	0.25	Represents very low relevance to the industry or user
Low	0.5	Represents low relevance to the industry or user
Medium	1	Represents medium relevance to the industry or user
High	2	Represents high relevance to the industry or user
Very high	4	Represents very high relevance to the industry or user

Source: WRI.

to water risks and the subjective nature of indicator weights made this technique an ideal fit. The results of the default weighting scheme can be found in the first column of Table 3.

Industry-specific weighting scheme

Additionally, we developed preset weighting schemes for nine industry sectors on the basis of information provided in corporate water disclosure reports and input from industry experts to reflect the risks and challenges faced by each water-intensive sector. For each industry, we modified the default indicator weights on the basis of the relative importance of each indicator to the industry using information disclosed by companies on their exposure to, and losses from, water-related risks. To validate the industry-sector preset weighting schemes, we presented preliminary weighting schemes to industry representatives from the nine sectors and solicited feedback on the relative importance of each indicator for their sector. The results can be found in Table 3.

Custom weighting scheme

In the online tool, users can specify their own custom weighting scheme.

Using the weighting schemes, grouped water risk scores can be calculated. The relative weight of each indicator is illustrated in Figure 7. The definition for each subgroup is listed below:

Physical Risk Quantity

Physical Risk Quantity measures risk related to too little or too much water by aggregating all selected indicators from the physical risk quantity category. Higher values indicate higher water quantity risks.

Physical Risk Quality

Physical Risk Quality measures risk related to water that is unfit for use by aggregating all selected indicators from the Physical Risk Quality category. Higher values indicate higher water quality risks.

Regulatory and Reputational Risk

Regulatory and Reputational Risk measures risk related to uncertainty in regulatory change, as well as conflicts with the public regarding water issues. Higher values indicate higher regulatory and reputational water risks.

Finally, the three grouped water risk scores can be used to determine the overall water risk score. The sums of the weights are used to calculate the relative contribution of each group.

Overall Water Risk

Overall Water Risk measures all water-related risks, by aggregating all selected indicators from the Physical Risk Quantity, Physical Risk Quality, and Regulatory and Reputational Risk categories. Higher values indicate higher water risk.

LIMITATIONS

Not every aspect of water risk has usable global data sets enabling it to be incorporated into our framework. Certain important elements are partially missing from the framework, such as water management and governance.³⁰

The local social dimensions of water risks are not incorporated into this framework and database. Policy, regulation, and response to water crises are paramount in estimating water risks and fully understanding their impacts. In the end, each region or location's ability to cope with water-related issues will affect its water risk.

Several limitations are associated with the framework (composite index) approach. First, it requires mapping the indicators to comparable (0–5) scale, thereby losing information such as absolute values. The second limitation, linked to the first, is that we combined data with various spatial and temporal resolutions and ranges into a single framework. Third, there are only two

and three indicators in the quality and regulatory and reputational groups, respectively. This makes these groups sensitive to errors in the underlying data. We provide industry and custom weighting to mitigate this limitation, but this requires the user to understand the data. The framework's water quality indicators do not reflect the full range of water quality threats but focus on nutrient pollution. The framework does not endorse framing water-quality solutions solely around coastal eutrophication or municipal wastewater. A fourth limitation of the framework approach is the mixing of risk types. The framework is inconsistent in including the exposure and vulnerability layers for all indicators.

In addition to the limitations of the framework approach, each indicator's baseline and future projections come with its own limitations. For the indicator-and-projection-specific limitations, please see the relevant sections above and the associated literature. Since many of the indicators rely on the PCR-GLOBWB 2 hydrological model and HydroBASINS 6 (hydrological sub-basins), some of these specific limitations are copied below.

Coastal sub-basins and islands in HydroBASINS 6 are often grouped for various reasons explained in Lehner et al. (2008). This grouping is coarse and results in inaccuracies, primarily when water demand can be satisfied using remote water supply.

PCR-GLOBWB 2 has no means to model interbasin transfer. Interbasin transfer happens when demand in one sub-basin is satisfied with supply from another sub-basin that is not upstream. Many major metropolitan areas source their water from adjacent sub-basins. Thus, baseline water stress in a given sub-basin may at times appear worse than it is where interbasin transfers are available to meet demand in that sub-basin. Alternatives to the moving window size and regression method used to process the PCR-GLOBWB 2 results could not be assessed due to the lack of validation data.

Direct validation of the aggregated grouped water risks and overall water risk is not possible. The perception of water risk is subjective, and robust validation methods for multi-indicator frameworks are unavailable.

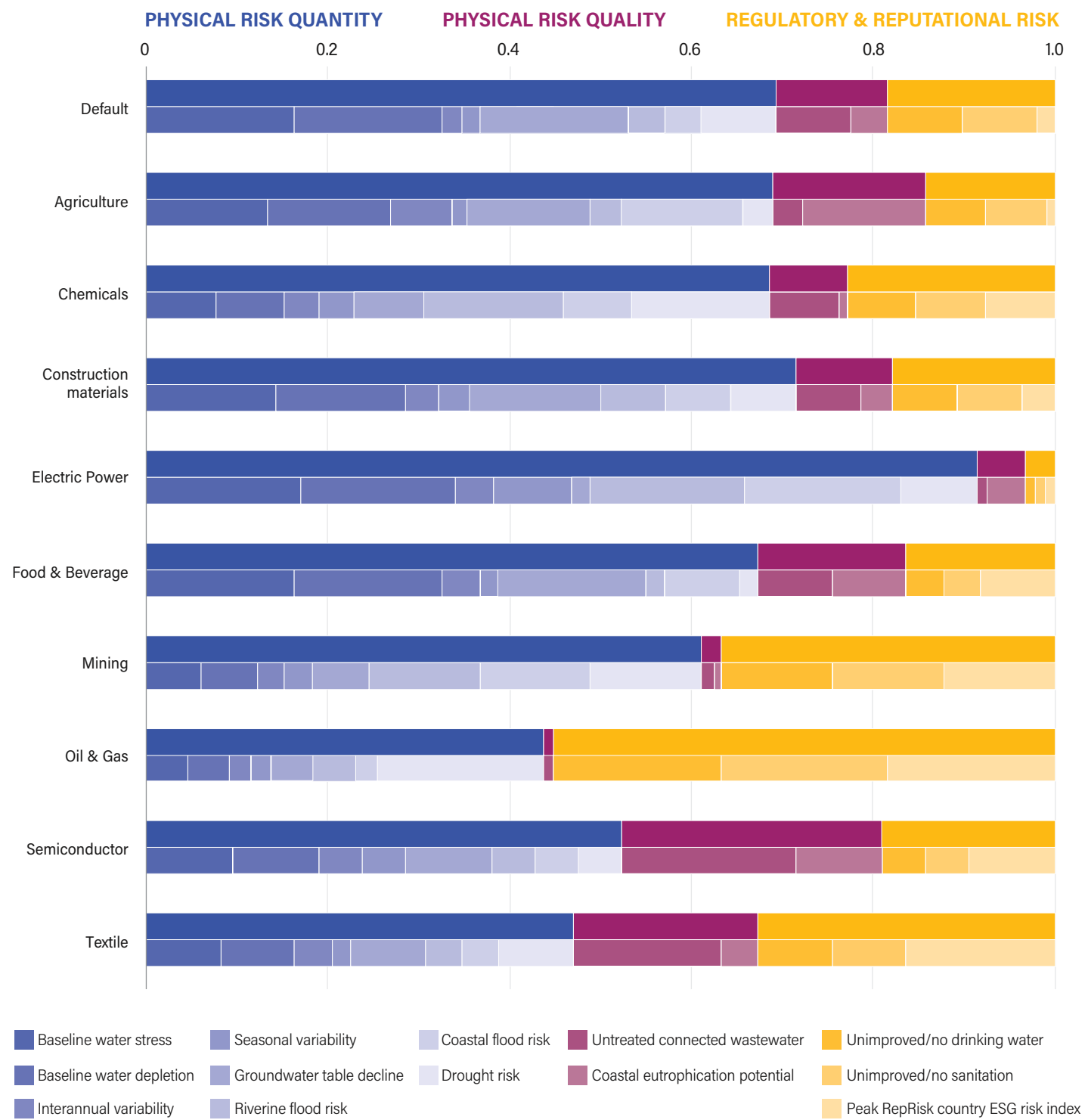
It is crucial to understand what the Aqueduct 4.0 framework and database can and cannot do. Aqueduct 4.0 is tailored to comparing regions on a larger scale. It has limited application at a local level. The presented results should therefore be used as a prioritization tool, after which deeper dive assessments should be used to understand local conditions with greater accuracy.

Table 3 | Industry or user relevance weights and their descriptions

		DEFAULT	AGRICULTURE	CHEMICALS	CONSTRUCTION MATERIALS	ELECTRIC POWER	FOOD AND BEVERAGE	MINING	OIL AND GAS	SEMICONDUCTOR	TEXTILE
PHYSICAL RISK QUANTITY	1	Baseline water stress	4	4	2	2	4	4	2	1	2
	2	Baseline water depletion	4	4	2	2	4	4	2	1	2
	3	Interannual variability	0.5	2	1	2	1	1	2	1	2
	4	Seasonal variability	0.5	0.5	1	0.5	2	0.5	1	0.5	1
	5	Groundwater table decline	4	4	2	2	0.5	4	2	1	2
	6	Riverine flood risk	1	1	4	1	2	0.5	4	1	1
	7	Coastal flood risk	1	1	4	1	4	0.5	4	4	1
	8	Drought risk	2	4	2	1	4	2	4	0.5	1
PHYSICAL RISK QUALITY	9	Untreated connected wastewater	2	1	2	1	0.25	2	0.5	0.25	4
	10	Coastal eutrophication potential	1	4	0.25	0.5	1	2	0.25	0	2
REGULATORY AND REPUTATIONAL RISK	11	Unimproved/no drinking water	2	2	2	1	0.25	1	4	4	1
	12	Unimproved/no sanitation	2	2	2	1	0.25	1	4	4	1
	13	Peak RepRisk country ESG risk index	0.5	0.25	2	0.5	0.25	2	4	4	2

Source: WRI.

Figure 8 | Indicator weights per industry



Notes: Weights are based on data availability. Masked or NoData values are excluded from the aggregated weighting. Please see the online tool for the results. The data are also available for download.

Source: WRI.

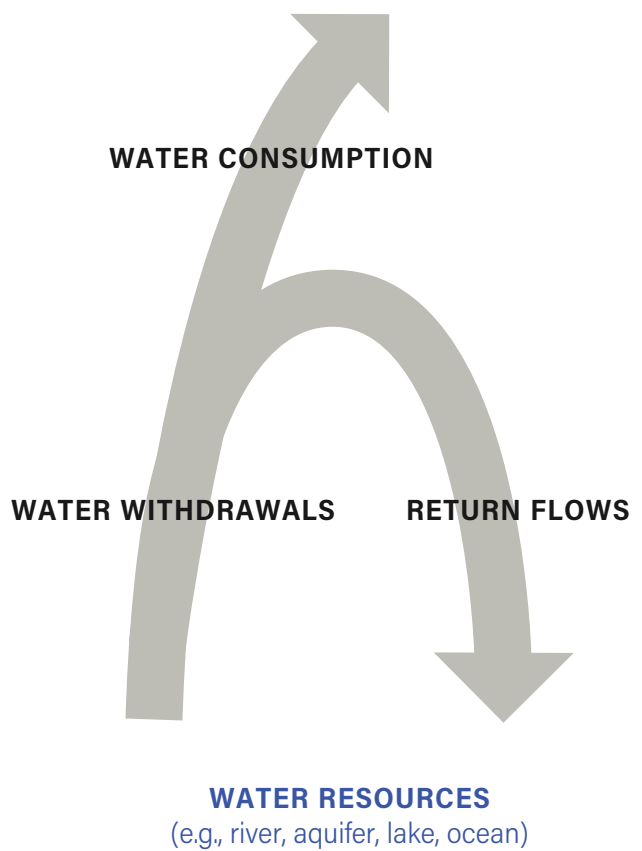
APPENDIX A: DEMAND, WITHDRAWAL, AND RETURN FLOW

This appendix describes the hydrological terminology used in PCR-GLOBWB 2. An overview is shown in Figure A1. PCR-GLOBWB 2 determines water demand. Withdrawal is demand limited by available water.

Withdrawal consists of two components: Consumptive withdrawal and nonconsumptive withdrawal. Gross withdrawal refers to consumptive plus nonconsumptive withdrawal. Net withdrawal refers to only the consumptive withdrawal.

The nonconsumptive withdrawal will return to the water body, usually downstream, and is also referred to as return flow.

Figure A1 | **Schematic of demand, gross and net withdrawal, and return flow**



Source: WRI.

APPENDIX B: GEOGRAPHIC CONVERSION TABLE

Table B1 is intended to provide a quick and approximate sense of scale

Table B1 | Common arc lengths

ARC LENGTH	DECIMAL DEGREES	DISTANCE AT EQUATOR (KM)	APPROXIMATE DISTANCE AT EQUATOR (KM)
360 arc degrees	360	40,030.17	40,000
1 arc degree	1	111.19	110
30 arc minutes	0.5	55.60	55
5 arc minutes	0.08333	9.27	10
1 arc minute	0.016667	1.85	2
30 arc seconds	0.008333	0.93	1
15 arc seconds	0.004167	0.46	.5

Source: WRI

APPENDIX C: PCR-GLOBWB 2

Water stress, water depletion, interannual variability, seasonal variability, groundwater table decline, and elements of the flood risk indicators are all based on the PCRaster Global Water Balance 2 model (PCR-GLOBWB 2) (Sutanudjaja et al. 2018; Sutanudjaja et al. 2023).

This appendix covers the basic model structure of PCR-GLOBWB 2 and the settings used for the Aqueduct run.

For baseline water stress, baseline water depletion, interannual variability, and seasonal variability we used a setup with default groundwater configuration. We will refer to this run as the default PCR-GLOBWB 2 run.

For the groundwater table decline indicator, we used a setup of PCR-GLOBWB 2 with an advanced representation of groundwater based on MODFLOW (de Graaf et al., 2017). We will refer to this setup as the PCR-GLOBWB 2 + MODFLOW run.

Digital elevation model

The starting point of almost any hydrological model and analysis is a digital elevation model (DEM). The DEM will determine the runoff direction; that is, the way the water flows. Aqueduct uses the same DEM as PCR-GLOBWB 2 and is a combination of the 30 × 30 arc second HydroSheds data (Lehner et al. 2008) with the 3 × 3 arc second Multi-Error-Removed Improved-Terrain Hydro Digital Elevation Model (MERIT Hydro DEM) (Yamazaki et al. 2019). Lakes and wetlands from the Global Lakes and Wetlands Database (GLWD) (Lehner and Döll 2004a) are extracted. Finally, reservoirs and dams from the Global Reservoir and Dam (GRanD) database have been used (Lehner et al. 2011). In short, lakes and reservoirs are part of PCR GLOBWB 2's drainage network, meaning their storage is actively updated through the routing network. Lake outflow uses a standard storage-outflow relationship (Bos, 1989); reservoir flow follows a release strategy based on the average passing discharge (limited by the minimum and maximum storage per each reservoir's construction year). Lake and reservoir storage is subject to abstraction from both evaporation and human withdrawals. The result is a hydrologically corrected data set of elevation, resampled to the PCRGLOBWB resolution of 5 × 5 arc minutes (approximately 10 km at the equator).

Local drainage direction

The local drainage direction, or the way water flows from one grid cell to the next, is derived from the DEM and assumes a strictly convergent flow. This means that in PCR-GLOBWB 2 and Aqueduct, bifurcations and river deltas are modeled as one stream instead of splitting rivers.

Model structure

PCR-GLOBWB 2 is a grid-based, modular global hydrological model. The world is represented by a 4,320 × 2,610 grid with a resolution of 5 × 5 arc minutes. For each of these cells, the model contains the following modules:

- Meteorological forcing
- Land surface
- Groundwater
- Surface water routing
- Irrigation and water use

See Figure C1 for a schematic representation of the model.

Meteorological forcing module

To model key weather elements that affect hydrology, the meteorological forcing of PCR-GLOBWB 2 uses daily time series of spatial fields of precipitation, temperature, and reference evaporation.

The default run is forced using data from two data sources: Global Soil Wetness Project Phase 3 (GSWP3) v1.09 (Dirmeyer et al. 2006) for the period 1960–78 and W5E5 (which merges WATCH Forcing Data with ERA5³¹ (WFDE5)) to extend the analysis to 2019 (Lange et al. 2021).

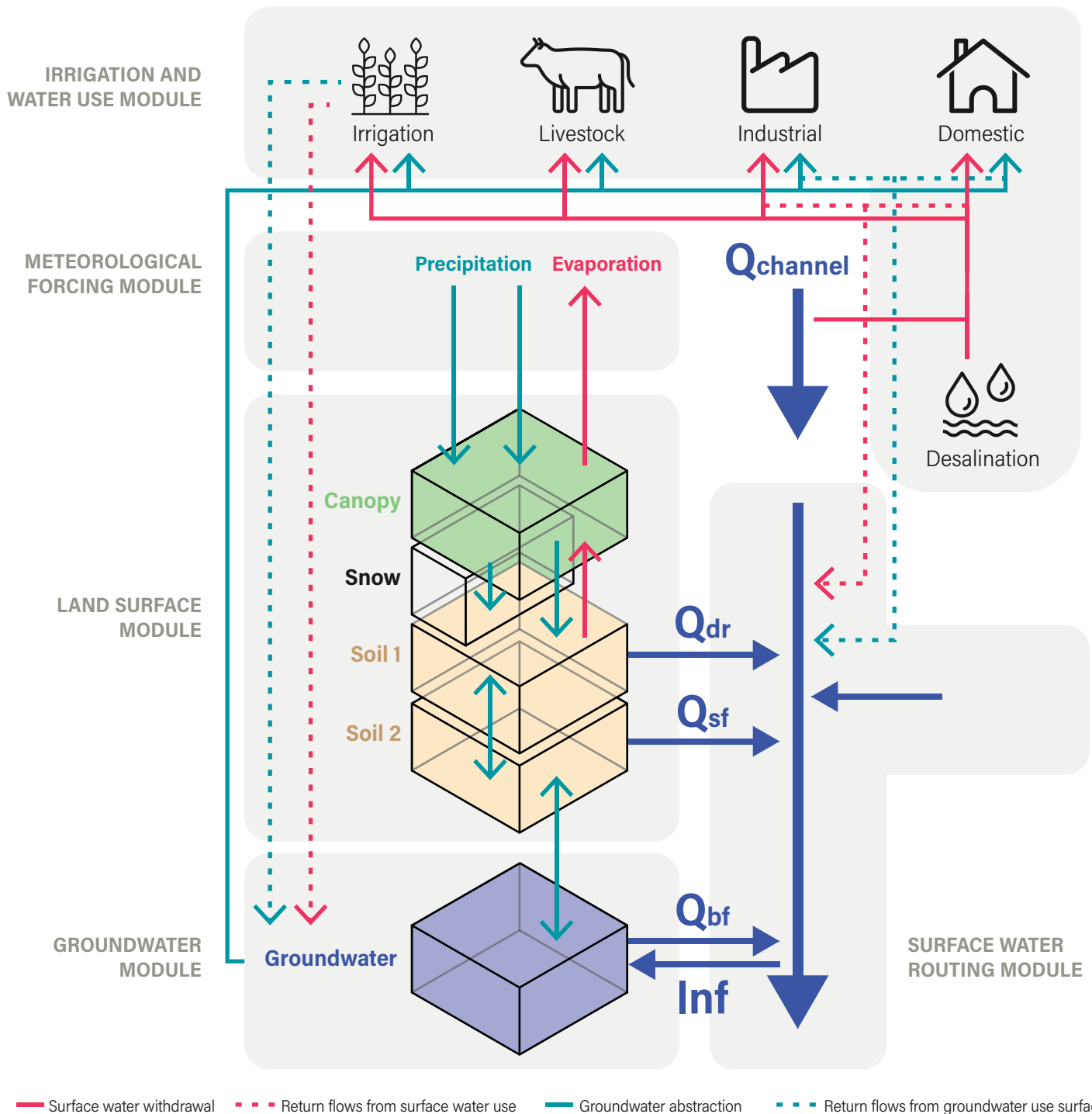
Reference evapotranspiration is calculated using Penman-Monteith, according to the FAO guidelines (Allen et al. 1998).

For groundwater, the PCR-GLOBWB 2 + MODFLOW run is forced using combined Climatic Research Unit (CRU) and Era-Interim (Harris et al. 2014; Dee et al. 2011). Although the model ran for 1959–2015, only the results for 1990–2014 have been used to calculate the groundwater table decline indicator (Verdin and Greenlee 1996).

Land surface model

This is the central module of PCR-GLOBWB 2 and connects directly to all other modules. It consists of multiple vertically stacked layers: canopy, snow, soil layer 1 (S1), and soil layer 2 (S2). See Figure C1. There are vertical fluxes between the stacked layers (e.g., S1 to S2 and vice versa), as well as with the climate forcing module (e.g., precipitation and evaporation) and the groundwater module (e.g., S2 to groundwater). Furthermore, there are horizontal fluxes to the runoff

Figure C1 | PCR-GLOWB 2 schematic overview



Note: "Schematic overview of a PCR-GLOWB 2 cell and its modeled states and fluxes. S1, S2 (soil moisture storage), S3 (groundwater storage), Qdr (surface runoff—from rainfall and snowmelt), Qsf (interflow or stormflow), Qbf (baseflow or groundwater discharge), and Inf (riverbed infiltration from to groundwater). The thin red lines indicate surface water withdrawal, the thin blue lines groundwater abstraction, the thin red dashed lines return flows from surface water use, and the thin dashed blue lines return flows from groundwater use surface. For each sector, withdrawal – return flow = consumption. Water consumption adds to total evaporation. In the figure, the five modules that make up PCR-GLOWB 2 are portrayed on the model components" (Sutanudjaja et al. 2018).

Source: Based on raw data from Sutanudjaja et al. (2018), modified/aggregated by WRI.

module. Within each grid cell, subgrid variability is modeled using a land-use class approach. This means that each grid cell is assigned a fraction of four land-use classes:

- Tall natural vegetation
- Short natural and nonnatural (rainfed crops) vegetation
- Nonpaddy-irrigated crops
- Paddy-irrigated crops (e.g., wet rice)

For instance, a grid cell might consist of 20 percent tall natural vegetation, 25 percent short vegetation, 40 percent nonpaddy-irrigated crops, and 15 percent paddy-irrigated crops (total 100 percent). Soil and vegetation parameters are obtained for each class and for each grid cell. Hence the soil and vegetation conditions are spatially distributed.

The Global Land Cover Characteristics Data Base, version 2.0 ("GLCC 2.0" 2010) and land surface parameter data set (Hagemann 2002) are used to assign the four land-use classes to each 5 arc minute grid cell as well as obtain a few soil and vegetation parameters.

For each of the four land-use classes and for each soil layer (S1 and S2), the remaining soil parameters are defined using SoilGrids250 (Hengl et al., 2017) and the WISE data set on global soil properties (Batjes 2012). SoilGrids250 was used to replace the Digital Soil Map of the World (Nachtergael et al. 2009) because of its finer resolution.

Finally, additional monthly vegetation properties, including leaf area index (LAI) and crop factors, are derived from the MIRCA 2000 data set (Portmann et al. 2010) and the Global Crop Water Model (Siebert and Döll 2010). For each of the four land-use classes, the following evaporative fluxes are defined:

- Interception evaporation
- Bare soil evaporation
- Snow sublimation
- Vegetation-specific transpiration

Another main building block in the land surface model is runoff and infiltration modeling. There are two runoff components in the land surface module: (1) direct runoff from soil layer 1 combined with snowmelt from the snow layer and (2) stormflow19 runoff from soil layer 2.

Direct and stormflow runoff are determined by excess infiltration according to the advanced ARNO scheme approach (Todini 1996; Hagemann and Gates 2003). This scheme determines which fraction will transfer vertically (infiltration) or horizontally (runoff).

APPENDIX D: DELTA SUB-BASINS

The underlying digital elevation models of PCR-GLOBWB 2 and HydroBASINS assume a strictly convergent flow, which in some cases leads to erroneous results. Rivers will sometimes bifurcate, especially in flat delta areas. Available water resources and water withdrawal are pooled within each sub-basin. Therefore, sub-basins that are part of the same delta need to be grouped and assumed to belong to a common hydrological unit.

The previous version of Aqueduct uses sub-basins derived from the Global Drainage Basin Database (GDBD) (Masutomi et al. 2009). By default, GDBD does not contain information about which basins were grouped. According to the author of GDBD, it is not possible to replicate the delta grouping using the HydroBASINS data set. Therefore, additional information regarding the 67 delta basins in GDBD was obtained directly from the authors and joined to the original database.

The process of finding and grouping delta HydroBASINS includes a semiautomated way to create a shortlist for potential delta sub-basins, and a manual step to ensure the correct classification.

To classify HydroBASINS into delta regions, a spatial join was performed between HydroBASIN level 6 and GDBD with delta classifier information. The HydroBASINS that intersect the GDBD delta basins are put on a shortlist for further inspection.

The second step is to count the number of separate GDBD streams in each sub-basin. Multiple streams are an indication for delta sub-basins.

As a third step, each shortlisted delta sub-basin is manually checked by comparing the shortlisted sub-basins with all water bodies extracted from OpenStreetMaps and the flow direction and flow accumulation of both HydroBASINS and PCR-GLOBWB 2 (OpenStreetMap contributors 2018; Lehner and Grill 2013; Sutanudjaja et al. 2018).

In total, 196 HydroBASINS are grouped into 63 delta basins. Eighty-nine delta regions have been examined. A column containing delta information is added to the final Aqueduct database.

ENDNOTES

1. We used time series of groundwater heads. Groundwater head is a measure of pressure and can be linked to groundwater tables. See the groundwater table decline indicator for more information.
2. See Appendix A for the terminology.
3. Gross demand is the maximum potential water requirement, compared to withdrawals, which represents the actual amount of water used. For example, a given year may use fewer withdrawals if heavy precipitation satisfied the water requirements. See Appendix A for more details.
4. Water use estimates for domestic, industrial, and livestock sectors are inputs to PCR-GLOBWB 2. Irrigation is the only sectoral demand that is an output of PCR-GLOBWB 2. Irrigation demand is a function of crop extents and climatic conditions such as temperature and humidity, and is therefore calculated on-the-fly during the modeling process (to adjust to the climate forcing data). For example, a crop field will require more water during a hotter summer than a cooler summer.
5. Consumption from irrigation is calculated by taking the portion of precipitation lost to evaporation.
6. We assume that all water withdrawn for livestock is consumed. Therefore, livestock net consumption equals livestock gross demand.
7. Interflow is the flow of water in the unsaturated ground below the surface but above the groundwater level. It discharges to above-ground streams rather than infiltrates into groundwater.
8. The PCR-GLOBWB2 output is called "runoff". It is the sum of direct runoff, interflow, and base flow within the catchment. Consumption is not removed. For more detail, see Appendix C.
9. The PCR-GLOBWB2 output is called "river discharge". It is the accumulative flow of direct runoff, interflow and base flow, minus water consumption (i.e., surface water abstraction—return flow). Evaporation from river and infiltration from river to groundwater are also removed from the accumulated flow. For more detail, see Appendix C.
10. Water that is being transported from one basin to another other than natural flow.
11. Using the World Eckert IV projection.
12. Aqueduct 3.0 rescaled data to a 30 arc second resolution. However, with the inclusion of the 15 future projections runs, Aqueduct 4.0 had about 43x more data to process; therefore, we experimented with different resampling sizes, assessing both the run time and change in results. We found that by using a 1 arc minute resolution, we could run the spatial reduction twice as fast while introducing minimal changes in the results.
13. An inflow point is where the stream enters the catchment for the first time and is completely upstream of the catchment (there is no presence of the catchment in its upstream path); an output point is where the stream leaves the catchment, and there is no presence of the catchment in its downstream path.
14. LDD is at the same 5 x 5 arc minute resolution as discharge data.
15. Rasterization is the process of turning a polygon into a grid (i.e., a series of squares). Polygons may have rounded edges, which can get lost in the rasterization process. Location boundaries, such as sub-basins and state borders, are polygons, whereas hydrological data, such as discharge, exist in a gridded format.
16. PCR-GLOBWB 2 uses a 5 x 5 arc minute spatial resolution, whereas HydroBASINS sub-basins are derived from a much finer digital elevation model (3 x 3 arc seconds) resampled to 15 x 15 arc second resolution. The result is that the larger 5 x 5 arc minute grid cells might (partially) overlap adjacent sub-basins, thereby erroneously making water available to that sub-basin.
17. Discharge represents cumulative flow. Although a false output point may temporarily show flow into an adjacent sub-basin, it is not contributing to that basin's accumulated flow because they are not hydrologically connected.
18. Years prior to 1979 (1960–1978) are no longer included in the baseline because they use a different reference climate forcing dataset than the more recent years. Data from 1979 to 2019 use W5E5 (Lange et al. 2021) for its observed atmospheric climate forcing data. Data from 1960 to 1978 use Global Soil Wetness Project Phase 3 (GSWP3) v1.09 (Dirmeyer et al. 2006).
19. The irrigation is especially sensitive to climate forcing and evapo-transpiration algorithm limitations.
20. The Theil-Sen regressor is a non-parametric method for linear regression that uses the median slope between points to estimate trend (Sen 1968). It is particularly powerful at handling outliers, which is why we use it over the Ordinary Least Sum regressor.

21. Baseline water stress and baseline water depletion use a fraction approach. When the denominator is very close to zero, the value will be extremely high and is often based on only a few data points. Please see the "Indicator" section and the respective equations.
22. Bias-corrected data for these GCMs are available under the ISI-MIP 3b protocol (ISIMIP 3 Protocol 2021).
23. The computation resources for running the model and storing its outputs limited us to 5 GCM runs per scenario.
24. Environmental flow requirements are implicitly considered in the thresholds.
25. 5 x 5 arc minute.
26. Our research partners at Deltares and Utrecht University ran the model for 1960–2014, but only 1990–2014 has been used to calculate the indicator. The reason is that groundwater development began to increase in the late 1980s and 1990s in some countries that use groundwater intensively. We assume this period to be representative of the current trend; however, further optimization might provide better insights as to the best range. Although this is different from some other indicators, we are consistently calculating baseline scores, thereby making it possible to aggregate various temporal ranges.
27. The vulnerability of people to floods is assessed as a binary condition: they are either flooded or they are not.
28. The vulnerability of people to floods is assessed as a binary condition: they are either flooded or they are not.
29. Water use estimates for domestic, industrial, and livestock sectors are inputs to PCR-GLOBWB 2. Irrigation is the only sectoral demand that is an output of PCR-GLOBWB 2. Irrigation demand is a function of crop extents and climatic conditions such as temperature and humidity and is therefore calculated on-the-fly during the modeling process (to adjust to the climate forcing data). For example, a crop field will require more water during a hotter summer than a cooler summer.
30. These elements are indirectly covered in the Regulatory and Reputational Risk group.
31. WATCH (WATer and global CHange); ERA5 (ECMWF Re-Analysis fifth generation); ECMWF (European Centre for Medium-Range Weather Forecasts).

REFERENCES

- Allen, R.G., L.S. Pereira, D. Raes, M. Smith, and others. 1998. "Crop Evapotranspiration: Guidelines for Computing Crop Water Requirements." FAO Irrigation and Drainage Paper 56.
- "AQUASTAT." n.d. <http://www.fao.org/nr/water/aquastat/main/index.stm>. Accessed February 13, 2019.
- Arias, P., N. Bellouin, E. Coppola, R. Jones, G. Krinner, J. Marotzke, V. Naik, M. Palmer, G.-K. Plattner, J. Rogelj, M. Rojas, J. Sillmann, T. Storelvmo, P. Thorne, B. Trewin, K. Rao, B. Adhikary, R. Allan, K. Armour, K. Zickfeld, 2021. IPCC AR6 WGI Technical Summary. pp. 33–144. <https://doi.org/10.1017/9781009157896.002>.
- Batjes, N.H. 2012. "ISRIC-WISE Derived Soil Properties on a 5 by 5 Arc-Minutes Global Grid (Ver. 1.2)." ISRIC-World Soil Information.
- BGR and UNESCO (Bundesanstalt für Geowissenschaften und Rohstoffe and United Nations Educational, Scientific, and Cultural Organization). 2018. "Groundwater Resources of the World." https://www.whymap.org/whymap/EN/Maps_Data/Gwrw/gwrw_node_en.html.
- Billen, G., and J. Garnier. 2007. "River Basin Nutrient Delivery to the Coastal Sea: Assessing Its Potential to Sustain New Production of Non-siliceous Algae." *Marine Chemistry* 106 (1–2): 148–60. doi:10.1016/j.marchem.2006.12.017.
- Bouwman, A., T. Kram, and K. Klein Goldewijk. 2006. "Integrated Modelling of Global Environmental Change: An overview of IMAGE4." PBL Netherlands Environmental Assessment Agency, September 11.
- Bouwman, A.F., A.H.W. Beusen, J.A. Harrison, and D.C. Reed. 2015. "Nutrient Release in Global Coastal Marine Ecosystems, and Modeling of Impacts (Hypoxia, Harmful Algal Blooms and Fisheries) in Relation to Coastal Conditions." Global Foundations for Reducing Nutrient Enrichment and Oxygen Depletion from Land Based Pollution, in Support of Global Nutrient Cycle. Global Environment Facility, United Nations Development Programme, and Intergovernmental Oceanographic Commission. <https://www.thegef.org/project/global-foundations-reducingnutrient-enrichment-and-odflb-pollution-support-gnc>.
- Brauman, K.A., B.D. Richter, S. Postel, M. Malsy, and M. Flörke. 2016. "Water Depletion: An Improved Metric for Incorporating Seasonal and Dry-Year Water Scarcity into Water Risk Assessments." *Elementa: Science of the Anthropocene* 4 (January): 000083. doi:10.12952/journal.elementa.000083.

- Carrão, H., G. Naumann, and P. Barbosa. 2016. "Mapping Global Patterns of Drought Risk: An Empirical Framework Based on Sub-national Estimates of Hazard, Exposure and Vulnerability." *Global Environmental Change* 39 (July): 108–24. doi: 10.1016/j.gloenvcha.2016.04.012.
- Dalkey, N., and O. Helmer. 1963. "An Experimental Application of the DELPHI Method to the Use of Experts." *Management Science* 9 (3): 458–67. doi:10.1287/ mnsc.9.3.458.
- Dirmeyer, P., X. Gao, M. Zhao, Z. Guo, T. Oki, N. Hanasaki, 2006. "GSWP-2: Multimodel Analysis and Implications for Our Perception of the Land Surface." *Bulletin of The American Meteorological Society* 87 (10): 1381--98. <https://doi.org/10.1175/BAMS-87-10-1381>.
- Dee, D.P., S.M. Uppala, A.J. Simmons, P. Berrisford, P. Poli, S. Kobayashi, U. Andrae, et al. 2011. "The ERA-Interim Reanalysis: Configuration and Performance of the Data Assimilation System." *Quarterly Journal of the Royal Meteorological Society* 137 (656): 553–97. doi:10.1002/qj.828.
- de Graaf, I., E. Sutanudjaja, L. Van Beek, and M. Bierkens. 2015. "A High-Resolution Global-Scale Groundwater Model." *Hydrology and Earth System Sciences* 19 (2): 823–37.
- de Graaf, I.E.M., R.L.P.H. van Beek, T. Gleeson, N. Moosdorf, O. Schmitz, E.H. Sutanudjaja, and M.F.P. Bierkens. 2017. "A Global-Scale Two-Layer Transient Groundwater Model: Development and Application to Groundwater Depletion." *Advances in Water Resources* 102 (April): 53–67. doi:10.1016/j.advwatres.2017.01.011.
- Doelman, J.C., E. Stehfest, A. Tabeau, H. van Meijl, L. Lassaletta, D.E.H.J. Gernaat, K. Hermans, M. Harmsen, V. Daioglou, H. Biemans, S. van der Sluis, D.P. van Vuuren, 2018. "Exploring SSP land-use dynamics using the IMAGE model: Regional and gridded scenarios of land-use change and land-based climate change mitigation." *Global Environmental Change* 48: 119–35. <https://doi.org/10.1016/j.gloenvcha.2017.11.014>
- Doorenbos, J., and W. Pruitt. 1977. "Crop Water Requirements." Irrigation and Drainage Paper No. 24. Rome: FAO (Food and Agriculture Organization of the United Nations).
- EOG and NOAA (Earth Observation Group and National Oceanic and Atmospheric Administration). n.d. "Nighttime Lights." NOAA. https://ngdc.noaa.gov/eog/viirs/_download_dnb_composites.html. Accessed February 13, 2019.
- Eisner, S. 2016. "Comprehensive Evaluation of the WaterGAP3 Model across Climatic, Physiographic, and Anthropogenic Gradients." PhD diss., University of Kassel.
- "FAOSTAT." 2012. FAO (Food and Agriculture Organization of the United Nations). <http://faostat.fao.org/>. Accessed February 12, 2019.
- "GADM Metadata." n.d. <https://gadm.org/metadata.html>. Accessed February 11, 2019.
- Galvis Rodríguez, S., E.H. Sutanudjaja, and M. Faneca Sánchez. 2017. "Memo: Update on the Groundwater Risk Indicators." Memo. Delft, the Netherlands: Deltares.
- Garnier, J., A. Beusen, V. Thieu, G. Billen, and L. Bouwman. 2010. "N:P:Si Nutrient Export Ratios and Ecological Consequences in Coastal Seas Evaluated by the ICEP Approach." *Global Biogeochemical Cycles* 24 (4). doi:10.1029/2009GB003583.
- Gassert, F., M. Luck, M. Landis, P. Reig, and T. Shiao. 2014. "Aqueduct Global Maps 2.1: Constructing Decision-Relevant Global Water Risk Indicators." World Resources Institute. https://wriorg.s3.amazonaws.com/s3fs-public/Aqueduct_Global_Maps_2.1-Constructing_Decision-Relevant_Global_Water_Risk_Indicators_final_0.pdf.
- Hagemann, S. 2002. "An Improved Land Surface Parameter Dataset for Global and Regional Climate Models." Max-Planck-Institut für Meteorologie, January. doi:10.17617/2.2344576.
- Hagemann, S., and L.D. Gates. 2003. "Improving a Subgrid Runoff Parameterization Scheme for Climate Models by the Use of High Resolution Data Derived from Satellite Observations." *Climate Dynamics* 21 (3–4): 349–59. doi:10.1007/s00382-003-0349-x.
- Harris, I., P.D. Jones, T.J. Osborn, and D.H. Lister. 2014. "Updated High-Resolution Grids of Monthly Climatic Observations: The CRU TS3.10 Dataset." *International Journal of Climatology* 34 (3): 623–42. doi:10.1002/joc.3711.
- Hartmann, J., and N. Moosdorf. 2012. "The New Global Lithological Map Database GLiM: A Representation of Rock Properties at the Earth Surface." *Geochemistry, Geophysics, Geosystems* 13 (12). <https://agupubs.onlinelibrary.wiley.com/doi/10.1029/2012GC004370>.
- Hempel, S., K. Frieler, L. Warszawski, J. Schewe, F. Piontek, "A trend-preserving bias correction—the ISI-MIP approach." *Earth System Dynamics* 4: 219–36 (2013).
- Hengl, T., J.M. de Jesus, G.B.M. Heuvelink, M.R. Gonzalez, M. Kilibarda, A. Blagotić, W. Shangguan, M.N. Wright, X. Geng, B. Bauer-Marschallinger, M.A. Guevara, R. Vargas, R.A. MacMillan, N.H. Batjes, J.G.B. Leenaars, E. Ribeiro, I. Wheeler, S. Mantel, B. Kempen, 2017. "SoilGrids250m: Global gridded soil information based on machine learning." *PLOS ONE* 12, e0169748. <https://doi.org/10.1371/journal.pone.0169748>

- IGRAC (International Groundwater Resources Assessment Centre). n.d. "Global Groundwater Information System (GGIS)." <https://www.un-igrac.org/globalgroundwater-information-system-ggis>. Accessed February 13, 2019.
- IOC-UNESCO and UNEP (Intergovernmental Oceanographic Commission and United Nations Environment Programme). 2016. "Large Marine Ecosystems: Status and Trends." Nairobi: UNEP. <http://geft-wap.org/water-systems/largemarine-ecosystems>.
- Kraijenhoff van de Leur, D.A. 1958. "A Study of Non-steady Ground-water Flow with Special Reference to a Reservoir Coefficient." *De Ingenieur* 19: B87-B94.
- Lange, S., 2021. ISIMIP3b Bias Adjustment Fact Sheet. ISIMIP.
- Lange, S., C. Menz, S. Gleixner, M. Cucchi, G.P. Weedon, A. Amici, N. Bellouin, H. Müller Schmied, H. Hersbach, C. Buontempo, C. Cagnazzo, 2021. *WFDE5 over land merged with ERA5 over the ocean (W5E5 v2.0)*. <https://doi.org/10.48364/ISIMIP.342217>.
- Lehner, B., and P. Döll. 2004b. "Development and Validation of a Global Database of Lakes, Reservoirs and Wetlands." *Journal of Hydrology* 296 (1-4): 1-22. doi:10.1016/j.jhydrol.2004.03.028.
- Lehner, B., and G. Grill. 2013. "Global River Hydrography and Network Routing: Baseline Data and New Approaches to Study the World's Large River Systems." *Hydrological Processes* 27 (15): 2171-86.
- Lehner, B., K. Verdin, and A. Jarvis. 2008. "New Global Hydrography Derived from Spaceborne Elevation Data." *Eos, Transactions, American Geophysical Union* 89 (10): 93. doi:10.1029/2008EO100001.
- Lehner, B., C.R. Liermann, C. Revenga, C. Vörösmarty, B. Fekete, P. Crouzet, P. Döll, et al. 2011. "High-Resolution Mapping of the World's Reservoirs and Dams for Sustainable River-Flow Management." *Frontiers in Ecology and the Environment* 9 (9): 494-502.
- Luck, M., M. Landis, F. Gassert. 2015. "Aqueduct Water Stress Projections: Decadal Projections of Water Supply and Demand Using CMIP5 GCMs." Technical Note. Washington, DC: World Resources Institute. wri.org/publication/aqueduct-water-stress-projections.
- Masutomi, Y., Y. Inui, K. Takahashi, and Y. Matsuoka. 2009. "Development of Highly Accurate Global Polygonal Drainage Basin Data." *Hydrological Processes* 23 (4): 572-84. doi:10.1002/hyp.7186.
- Mayorga, E., S.P. Seitzinger, J.A. Harrison, E. Dumont, A.H.W. Beusen, A.F. Bouwman, B.M. Fekete, et al. 2010. "Global Nutrient Export from WaterSheds 2 (NEWS 2): Model Development and Implementation." *Environmental Modelling & Software* 25 (7): 837-53. doi:10.1016/j.envsoft.2010.01.007.
- Mekonnen, M.M. and A.Y. Hoekstra, 2012. "A Global Assessment of the Water Footprint of Farm Animal Products." *Ecosystems* 15, 401-415. <https://doi.org/10.1007/s10021-011-9517-8>.
- Meyer, V., D. Haase, and S. Scheuer. 2009. "Flood Risk Assessment in European River Basins—Concept, Methods, and Challenges Exemplified at the Mulde River." *Integrated Environmental Assessment and Management* 5 (1): 17-26. doi:10.1897/IEAM_2008-031.1.
- Müller Schmied, H., S. Eisner, D. Franz, M. Wattenbach, F.T. Portmann, M. Flörke, and P. Döll. 2014. "Sensitivity of Simulated Global-Scale Freshwater Fluxes and Storages to Input Data, Hydrological Model Structure, Human Water Use and Calibration." *Hydrology and Earth System Sciences* 18 (9): 3511-38. doi:10.5194/hess-18-3511-2014.
- Nachtergaele, F., H. van Velthuizen, L. Verelst, N. Batjes, K. Dijkshoorn, V. van Engelen, G. Fischer, et al. 2009. "Harmonized World Soil Database." Wageningen, the Netherlands: ISRIC.
- OpenStreetMap contributors. 2018. Planet Dump. <https://Planet.Osm.Org>.
- Paul, P.K., Y. Zhang, N. Ma, A. Mishra, N. Panigrahy, R. Singh, 2021. "Selecting hydrological models for developing countries: Perspective of global, continental, and country scale models over catchment scale models." *Journal of Hydrology* 600, 126561. <https://doi.org/10.1016/j.jhydrol.2021.126561>.
- Portmann, F.T., S. Siebert, and P. Döll. 2010. "MIRCA2000-Global Monthly Irrigated and Rainfed Crop Areas around the Year 2000: A New High-Resolution Data Set for Agricultural and Hydrological Modeling." *Global Biogeochemical Cycles* 24 (1). doi:10.1029/2008GB003435.
- Reig, P., T. Shao, and F. Gassert. 2013. "Aqueduct Water Risk Framework." Working paper. Washington, DC: World Resources Institute. https://wriorg.s3.amazonaws.com/s3fs-public/aqueduct_water_risk_framework.pdf.
- RepRisk. n.d. "RepRisk ESG Data Science and Quantitative Solutions." www.reprisk.com.
- Rodell, M., P.R. Houser, U. Jambor, J. Gottschalck, K. Mitchell, C.-J. Meng, K. Arsenault, et al. 2004. "The Global Land Data Assimilation System." *Bulletin of the American Meteorological Society* 85 (3): 381-94. doi:10.1175/BAMS-85-3-381.
- Rohwer, J., D. Gerten, and W. Lucht. 2007. *Development of Functional Irrigation Types for Improved Global Crop Modelling*. PIK Report.

- Rowe, G., and G. Wright. 1999. "The Delphi Technique as a Forecasting Tool: Issues and Analysis." *International Journal of Forecasting* 15 (4): 353–75. doi:10.1016/S0169-2070(99)00018-7.
- Sen, P.K., 1968. Estimates of the Regression Coefficient Based on Kendall's Tau. *Journal of the American Statistical Association* 63: 1379–89. <https://doi.org/10.2307/2285891>
- Scussolini, P., J.C.J.H. Aerts, B. Jongman, L.M. Bouwer, H.C. Winsemius, H. de Moel, and P.J. Ward. 2016. "FLOPROS: An Evolving Global Database of Flood Protection Standards." *Natural Hazards and Earth System Sciences* 16 (5): 1049–61. doi:10.5194/nhess-16-1049-2016.
- Shiklomanov, I. 1997. "Comprehensive Assessment of the Freshwater Resources of the World." Stockholm: World Meteorological Organization.
- Siebert, S., and P. Döll. 2010. "Quantifying Blue and Green Virtual Water Contents in Global Crop Production as Well as Potential Production Losses without Irrigation." *Journal of Hydrology* 384 (3–4): 198–217. doi:10.1016/j.jhydrol.2009.07.031.
- Steinfeld, H., P. Gerber, T.D. Wassenaar, V. Castel, M. Rosales, and C. de Haan. 2006. *Livestock's Long Shadow: Environmental Issues and Options*. Rome: FAO (Food and Agriculture Organization of the United Nations).
- Strahler, A.N. 1957. "Quantitative Analysis of Watershed Geomorphology." *Eos, Transactions, American Geophysical Union* 38 (6): 913–20.
- Sutanudjaja, E.H., R. van Beek, N. Wanders, Y. Wada, J.H.C. Bosmans, N. Drost, R.J. van der Ent, et al. 2018. "PCR-GLOBWB 2: A 5 Arcmin Global Hydrological and Water Resources Model." *Geoscientific Model Development* 11 (6): 2429–53. doi:10.5194/gmd-11-2429-2018.
- Sutanudjaja, E.H., R. van Beek, E. Saccoccia, S. Kuzma, T. Luo, and M.F.P. Bierkens. 2023. "Hydrological projection of future global water states with CMIP6." Utrecht University. <https://public.yoda.uu.nl/geo/UU01/YM7A5H.html>.
- Todini, E. 1996. "The ARNO Rainfall: Runoff Model." *Journal of Hydrology* 175 (1): 339–82. doi:10.1016/S0022-1694(96)80016-3.
- Triantaphyllou, E. 2010. *Multi-criteria Decision Making Methods: A Comparative Study*. Applied Optimization 44. Dordrecht, the Netherlands: Kluwer.
- UNEP (United Nations Environment Programme). n.d. "UNEP." <https://www.unenvironment.org/>. Accessed on February 28, 2019.
- Vanham, D., A.Y. Hoekstra, Y. Wada, F. Bouraoui, A. de Roo, M.M. Meekonen, W.J. van de Bund, et al. 2018. "Physical Water Scarcity Metrics for Monitoring Progress towards SDG Target 6.4: An Evaluation of Indicator 6.4.2 'Level of Water Stress.'" *Science of the Total Environment* 613–14 (February): 218–32. doi:10.1016/j.scitotenv.2017.09.056.
- van Huijstee, J., B. van Bemmel, A. Bouwman, and F. van Rijn. 2018. "Towards an Urban Preview: Modelling Future Urban Growth with 2UP." 3255. The Hague: PBL Netherlands Environmental Assessment Agency. <https://www.pbl.nl/en/publications/towards-an-urban-preview>.
- van Vuuren, D., P.P.L. Lucas, and H. Hilderink. 2007. "Downscaling Drivers of Global Environmental Change: Enabling Use of Global SRES Scenarios at the National and Grid Levels." *Global Environmental Change: Uncertainty and Climate Change Adaptation and Mitigation* 17 (1): 114–30. doi:10.1016/j.gloenvcha.2006.04.004.
- Verdin, K.L., and S. Greenlee. 1996. "Development of Continental Scale Digital Elevation Models and Extraction of Hydrographic Features." In *Proceedings, Third International Conference/Workshop on Integrating GIS and Environmental Modeling*, Santa Fe, New Mexico, 21–26.
- Vörösmarty, C.J., B.M. Fekete, M. Meybeck, and R.B. Lammers. 2000. "Global System of Rivers: Its Role in Organizing Continental Land Mass and Defining Land-to-Ocean Linkages." *Global Biogeochemical Cycles* 14 (2): 599–621. doi:10.1029/1999GB900092.
- Vörösmarty, C.J., C. Léveque, C. Revenga, R. Bos, C. Caudill, J. Chilton, E. Douglas, et al. 2005. *Millennium Ecosystem Assessment Volume 1: Conditions and Trends*, chap. 7, "Freshwater Ecosystems." Millennium Ecosystem Assessment 1: 165–207.
- Wada, Y., L.P.H. van Beek, and M.F.P. Bierkens. 2011a. "Modelling Global Water Stress of the Recent Past: On the Relative Importance of Trends in Water Demand and Climate Variability." *Hydrology and Earth System Sciences* 15 (12): 3785–808. doi:10.5194/hess-15-3785-2011.
- Wada, Y., L.P.H. van Beek, D. Viviroli, H.H. Dürr, R. Weingartner, and M.F.P. Bierkens. 2011b. "Global Monthly Water Stress: 2. Water Demand and Severity of Water Stress, 2." *Water Resources Research* 47 (7). doi:10.1029/2010WR009792.
- Wada, Y., D. Wisser, and M.F.P. Bierkens. 2014. "Global Modeling of Withdrawal, Allocation and Consumptive Use of Surface Water and Groundwater Resources." *Earth System Dynamics* 5 (1): 15–40. doi:10.5194/esd-5-15-2014.

- Wada, Y., M. Flörke, N. Hanasaki, S. Eisner, G. Fischer, S. Tramberend, Y. Satoh, M.T.H. van Vliet, P. Yillia, C. Ringler, P. Burek, D. Wiberg, 2016. "Modeling global water use for the 21st century: the Water Futures and Solutions (WFaS) initiative and its approaches." *Geoscientific Model Development* 9: 175–222. <https://doi.org/10.5194/gmd-9-175-2016>.
- Wang, D., K. Hubacek, Y. Shan, W. Gerbens-Leenes, J. Liu, 2021. "A Review of Water Stress and Water Footprint Accounting." *Water* 13, 201. <https://doi.org/10.3390/w13020201>.
- Ward, P.J., H.C. Winsemius, S. Kuzma, T. Luo, M.F.P. Bierkens, A. Bouwman, H. de Moel, et al. 2020. "Aqueduct Floods Methodology." Technical Note. Washington, DC: World Resources Institute.
- Wendling, Z.A., J.W. Emerson, D.C. Esty, M.A. Levy, and A. de Sherbinin. 2018. "2018 Environmental Performance Index." New Haven, CT: Yale Center for Environmental Law and Policy. <https://epi.envirocenter.yale.edu/2018-epi-report/> introduction.
- Wint, W., and T.P. Robinson. 2007. Gridded Livestock of the World, 2007. Rome: Food and Agriculture Organization of the United Nations.
- World Bank. n.d. "World Bank National Accounts Data." World Bank. <https://data.worldbank.org>. Accessed February 13, 2019.
- WHO and UNICEF (World Health Organization and United Nations Children's Fund). 2017. *Progress on Drinking Water, Sanitation and Hygiene: 2017 Update and SDG Baselines*. <https://washdata.org/>.
- WRI (World Resources Institute). n.d. WRI's Open Data Commitment: World Resources Institute. <https://www.wri.org/about/open-data-commitment>. Accessed February 27, 2019.
- WRI, UNEP, UNDP, and World Bank, eds. 1998. *World Resources, 1998–99: A Guide to the Global Environment Environmental Change and Human Health*. New York: Oxford University Press.
- Xie, H., C. Ringler, and G. Pitois. 2016. "Assessing Global BOD, Nitrogen and Phosphorus Loadings under Socioeconomic and Climate Change Scenarios." Technical note. IFPRI (International Food Policy Research Institute).
- Yamazaki, D., D. Ikeshima, J. Sosa, P. Bates, G. Allen, T. Pavelsky, 2019. "Hydro: A High-Resolution Global Hydrography Map Based on Latest Topography Dataset." *Water Resources Research* 55. <https://doi.org/10.1029/2019WR024873>.

ACKNOWLEDGEMENTS

We are pleased to acknowledge our institutional strategic partners, who provide core funding to WRI: Netherlands Ministry of Foreign Affairs, Royal Danish Ministry of Foreign Affairs, and Swedish International Development Cooperation Agency.

This publication was made possible thanks to the support of Microsoft, Moody's RMS, and Cargill Inc., and the Aqueduct Alliance (Accenture, Ansell, Cargill Inc., Ecolab Inc., Dutch Ministry of Infrastructure and Water Management, Gap, International Paper, Mars, Meta, Microsoft, Proctor & Gamble Company, Tyson Foods Inc., 3M). Additionally, we thank the World Bank for supporting parts of Aqueduct Floods.

The authors would like to thank the following people for providing invaluable insight and assistance in their reviews of this report: Zablon Adane (WRI), Courtnae Baily (WRI), Brittany Craig (Tyson Foods Inc.) and Homero Paltan Lopez (World Bank).

The authors would also like to thank our research partners at Deltares, IFPRI, IVM, RepRisk, and Utrecht University, as well as our WRI colleagues Nancy Sanchez, Carlos DelReal, Renee Pineda, Carlos Muñoz, Laura Malaguzzi Valeri, and Romain Warnault, for their extensive guidance and feedback during the design and development of this study.

Opinions or points of view expressed in this report are those of the authors and do not necessarily reflect the position of the reviewers, research partners, or the organizations they represent.

ABOUT THE AUTHORS

Samantha Kuzma is the data lead and senior manager for Global Water Data Products at World Resources Institute.
Contact: samantha.kuzma@wri.org

Marc F. P. Bierkens is a professor of hydrology at Utrecht University, where he holds the Chair of Earth Surface Hydrology in the Department of Physical Geography. He is also a senior scientist at Deltares.

Shivani Lakshman is a corporate water stewardship research analyst at the World Resources Institute.

Tianyi Luo is a director at Bluerisk.

Liz Saccoccia is a water security and geospatial associate at the World Resources Institute.

Edwin H. Sutanudjaja is the core developer of PCR-GLOBWB 2 in the Department of Physical Geography at Utrecht University.

Rens van Beek is an associate professor of large-scale hydrology and Earth surface processes at Utrecht University.

ABOUT WRI

World Resources Institute is a global research organization that turns big ideas into action at the nexus of environment, economic opportunity, and human well-being.

Our challenge

Natural resources are at the foundation of economic opportunity and human well-being. But today, we are depleting Earth's resources at rates that are not sustainable, endangering economies and people's lives. People depend on clean water, fertile land, healthy forests, and a stable climate. Livable cities and clean energy are essential for a sustainable planet. We must address these urgent, global challenges this decade.

Our vision

We envision an equitable and prosperous planet driven by the wise management of natural resources. We aspire to create a world where the actions of government, business, and communities combine to eliminate poverty and sustain the natural environment for all people.

Our approach

COUNT IT

We start with data. We conduct independent research and draw on the latest technology to develop new insights and recommendations. Our rigorous analysis identifies risks, unveils opportunities, and informs smart strategies. We focus our efforts on influential and emerging economies where the future of sustainability will be determined.

CHANGE IT

We use our research to influence government policies, business strategies, and civil society action. We test projects with communities, companies, and government agencies to build a strong evidence base. Then, we work with partners to deliver change on the ground that alleviates poverty and strengthens society. We hold ourselves accountable to ensure our outcomes will be bold and enduring.

SCALE IT

We don't think small. Once tested, we work with partners to adopt and expand our efforts regionally and globally. We engage with decision-makers to carry out our ideas and elevate our impact. We measure success through government and business actions that improve people's lives and sustain a healthy environment.



Copyright 2023 World Resources Institute. This work is licensed under the Creative Commons Attribution 4.0 International License.
To view a copy of the license, visit <http://creativecommons.org/licenses/by/4.0/>